

# LTE Synchronization Algorithms

D. S. Sridhar Reddy

EE11M01

A Thesis Submitted to  
Indian Institute of Technology Hyderabad  
In Partial Fulfillment of the Requirements for  
The Degree of Master of Technology



Department of Electrical Engineering

July 2013

## Declaration

I declare that this written submission represents my ideas in my own words, and where ideas or words of others have been included, I have adequately cited and referenced the original sources. I also declare that I have adhered to all principles of academic honesty and integrity and have not misrepresented or fabricated or falsified any idea/data/fact/source in my submission. I understand that any violation of the above will be a cause for disciplinary action by the Institute and can also evoke penal action from the sources that have thus not been properly cited, or from whom proper permission has not been taken when needed.

*D. S. Sridhar Reddy*

---

(Signature)

---

(D. S. Sridhar Reddy  
EE11M01)

---

(Roll No.)

## Approval Sheet

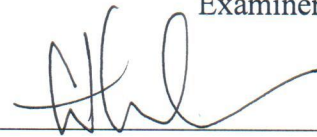
This thesis entitled "LTE Synchronization Algorithms" by D. S. Sridhar Reddy; EE11M01 is approved for the degree of Master of Technology from IIT Hyderabad.



Dr G. V. V. Sharma

Department of Electrical Engineering

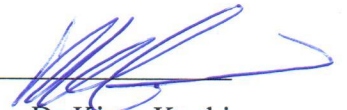
Examiner



Dr Sumohana Channappayya

Department of Electrical Engineering

Examiner



Dr Kiran Kuchi

Department of Electrical Engineering

Adviser

# Acknowledgements

# Dedication

# Abstract

Third Generation Partnership Project (3GPP) Long Term Evolution(LTE) provides high spectral efficiency, high peak data rates and frequency flexibility with low latency and low cost. Usage of modulation techniques like OFDMA and SC-FDMA enables LTE to achieve such requirements.However it is well known that OFDM systems like LTE are very sensitive when it comes to carrier frequency offsets and symbol synchronization errors.Inorder to transfer data correctly, the User Equipment(UE) must perform both uplink and downlink synchronization with the Base station(eNodeB). In this thesis, Primary Synchronization Signal(PSS) and Secondary Synchronization signal(SSS) are used to detect the cell-ID of the best serving base station and also to achieve downlink synchronization whereas Physical Random Access Channel(PRACH) preamble is used to obtain uplink synchronization. PSS and SSS helps to achieve downlink synchronization by estimating the frame timing and carrier frequency offsets.In this thesis a non-coherent detection approach is followed for detection of both PSS and SSS signals.

PSS is first detected in time domain by correlating with three reference PSS signals and then redundant information contained within the cyclic prefix enables to estimate the coarse symbol timing along with estimating the fractional carrier frequency offset. Frame synchronization and cell group ID(one among 168 groups) are obtained by detecting SSS signal in frequency domain. A non-coherent detection approach is followed in this thesis for SSS detection because of performance degradation in coherent detection approach for SSS detection because of channel difference between PSS and SSS. Integer carrier frequency offsets is estimated after SSS signal detection in frequency domain. Channel estimation is also performed on PSS and SSS signals after cell search and downlink synchronization. Inorder for the UE to be uplink synchronized with the best possible serving base station(eNodeB), the propagation delay of that given UE should be known to the eNodeB so that there are no misalignment of the frames of different UE's at the eNodeB. Both full frequency domain and hybrid time-frequency approach have been followed for PRACH detection at eNodeB. All algorithms are evaluated under multipath channel conditions and an initial carrier frequency mismatch and simulation results along with results pertaining to real time RF captured data have been obtained.

# Contents

# Chapter 1

## Introduction

In recent years the need for high quality, high data rate mobile multimedia transmission and throughput has been increasing. 3GPP Long Term Evolution (LTE) systems achieves this requirement by providing higher frequency efficiency and higher throughput with low latency and low cost. LTE can achieve peak data rates upto 300 Mbps in the downlink and data rate upto 75 Mbps in the uplink. Air interface based on Orthogonal Frequency Division Multiple Access (OFDMA) in downlink and Single Carrier Frequency Division Multiple Access (SC-FDMA) in uplink are used in LTE which enables LTE to achieve high spectral efficiency, robust performance in frequency selective channel conditions, simple receiver architecture, etc.

### 1.1 Orthogonal Frequency Division Multiplexing

Orthogonal Frequency Division Multiplexing (OFDM) can be defined simply as a form of Multi carrier modulation (MCM) where its carrier spacing is selected so that each subcarrier is orthogonal to the other subcarriers. OFDM has gained lot of interest in wireless systems because of its various advantages in lessening the severe effects of frequency selective fading [?]. By dividing a wide band channel into narrowband flat fading subchannels, OFDM enables high-rate and high-speed transmission over frequency selective fading channels when compared to single carrier systems. A repetition of last few samples of OFDM symbol, called cyclic prefix gets appended at start of OFDM symbol, which helps to eliminate Inter Symbol Interference (ISI), which makes OFDM to have inherent robustness against multipath interference and hence makes it suitable to be implemented in wireless environments. OFDM is also computationally efficient by using FFT and IFFT techniques to implement the modulation and demodulation functions.



However, it is well known that OFDM systems are sensitive and vulnerable to time and frequency synchronization errors, hence require accurate synchronization for interference-free data reception. Carrier frequency offsets, which are caused by inherent stability of the Transmitter and receiver carrier frequency oscillator, can lead to severe system degradation due to Inter Carrier Interference (ICI). Symbol timing synchronization must also be achieved in order to avoid ISI [?]. Impairments caused by multipath channel can also lead to ICI and ISI problems in OFDM systems. Thus we address two problems in OFDM receivers, one problem is the unknown OFDM symbol timing and the other is to eliminate fractional and integer frequency offsets effect.

### 1.1.1 OFDM system description

Consider an OFDM system which consists of  $N$  subcarriers. Let  $X_i(k)$  for  $k=0,1,\dots,N-1$ , denote the  $N$  subcarriers symbols where  $i$  represents the OFDM symbol number and  $k$  represents the subcarrier number. At the transmitter, the  $N$  symbols are modulated onto the  $N$  subcarriers via an inverse FFT (IFFT). The cyclic prefix is also added in the guard in the guard interval in order to Inter Symbol Interference (ISI) due to multipath fading effect of the wireless channel. The transmitted signal can be represented as

$$s(t) = \sum_{i=-\infty}^{\infty} \sum_{k=0}^{N-1} X_i(k) \Upsilon_{i,k}(t) \quad (1.1)$$

where  $\Upsilon_{i,k}(t)$  is the subcarrier pulse. That is

$$\Upsilon_{i,k}(t) = \begin{cases} e^{j2\pi(k/T)(t-T_{cp}-iT_{sym})} & iT_{sym} \leq t < (i+1)T_{sym} \\ 0 & \text{else} \end{cases} \quad (1.2)$$

where  $T_{sym} = T + T_{cp}$  is the duration of whole OFDM symbol including the cyclic prefix (CP),  $1/T$  is the OFDM subcarrier spacing and  $T_{cp}$  is the cyclic prefix (CP) duration.

We assume the channel over which the signal is transmitted is a multipath fading channel, which can be represented as follows

$$h(\tau, t) = \sum_{l=0}^{L-1} h_l(t) \cdot \delta(\tau - \tau_l) \quad (1.3)$$

where  $h_l(t)$  represents complex gains,  $\tau_l$  are the path time delays and  $L$  is the total

number of paths. Time delay for initial path is assumed to be zero.

At the receiver, if we assume perfect OFDM synchronization, the received sampled signal can be written as

$$r(nT_s) = \sum_{l=0}^{L-1} h_l(nT_s) s(nT_s - \tau_l) + n(nT_s) \quad (1.4)$$

where  $T_s = T/N$  is the sampling time interval and  $n(nT_s)$  denotes the sampled white Gaussian noise. The cyclic prefix is first removed from received OFDM symbol samples, then the remaining  $N$  samples are transformed into frequency domain via an FFT. The FFT output can be represented by

$$Y_i(k) = X_i(k)H_i(k) + n_i(k) \quad \text{for } k = 0, 1, \dots, N-1 \quad (1.5)$$

where  $n_i(k)$  is a white complex Gaussian noise with variance  $\sigma^2$ . The channel frequency response at subcarrier frequency  $f_k = k/T$  can be written as

$$H_i(k) = \sum_{l=0}^{L-1} h_l(nT_s) e^{-j2\pi\tau_l(k/T)} \quad (1.6)$$

Generally we assume that the channel does not change during one OFDM symbol, and CP length is longer than channel maximum delay spread.

### 1.1.2 Effects of Synchronization error

In the above subsection synchronization errors effects are not considered and an ideal synchronization in OFDM receiver has been assumed. However, in practical scenario this is not the case. There is usually a carrier frequency offset,  $\Delta f_{off}$ , between transmitter and receiver due to mismatch between the transmitter and receiver oscillators or the channel Doppler frequency shift, leading to ICI. The same holds for the receiver sampling clock. The effect of carrier frequency offsets can be written as

$$r(nT_s) = \left( \sum_{l=0}^{L-1} h_l(nT_s) s(nT_s - \tau_l) \right) e^{j2\pi(\epsilon/T)nT_s} + n(nT_s) \quad (1.7)$$

where  $\Delta f_{off} = (\epsilon/T)$  represents carrier frequency offset which consists of both integer frequency offset and fractional frequency offset.

The symbol timing error  $e_\theta = \hat{\theta} - \theta_0$  where  $\theta_0$  represents the position of the first

sample in the OFDM symbol useful part and  $\hat{\theta}$  is the estimated symbol timing will also effect the system. In the sequel we assume that  $e_\theta, \hat{\theta}$  and  $\theta_0$  are all values normalized by the OFDM sample interval. In the guard interval, there is a certain range that is not affected by the previous symbol because of the channel time dispersion. As long as the FFT window starts from this range, the orthogonality between the different subcarriers will be maintained. A symbol timing error within this interval can just result in a phase rotation of every subcarrier symbol given by

$$Y_i(k) = e^{j2\pi(k/N)e_\theta} X_i(k)H_i(k) + n_i(k), \quad (-T_{cp} + T_m)/T_s < e_\theta < 0 \quad (1.8)$$

where  $T_m$  is the channel maximum delay spread. If the beginning of the FFT window is out of the ISI free interval, however, the resulting ISI will destroy the orthogonality of the subcarriers. For instance, the demodulator output can be written as [?]

$$Y_i(k) = e^{j2\pi(k/N)e_\theta} \frac{N - e_\theta}{N} X_i(k)H_i(k) + n_i(k) + n_{e_\theta}(i, k), \quad e_\theta > 0 \quad (1.9)$$

where the ISI-induced ICI is modeled as additional noise  $n_{e_\theta}(i, k)$ . Thus, symbol synchronization must be so accurate that  $n_{e_\theta}$  is much smaller than  $n_i(k)$  and that the extra channel estimation error created by the symbol timing errors is also small.

The receiver sampling clock can sample at a sampling time interval  $\hat{T}_s$  which is different from  $T_s$  leading to sampling clock errors. The sampling clock errors include the clock phase error and the clock frequency error. The clock phase error effects are similar to the symbol timing errors and hence the clock phase errors can be treated as a kind of the symbol timing errors. The sampling clock frequency errors can cause the ICI. The normalized sampling frequency offset is given as  $\varsigma = (\hat{T}_s - T_s)/T_s$ . The effect of sampling clock offset can be written as

$$Y_i(k) = e^{j2\pi k\varsigma(T_{sym}/T)} \text{sinc}(k\varsigma) X_i(k)H_i(k) + n_i(k) + n_\varsigma(i, k) \quad (1.10)$$

where  $\text{sinc}(x) = \sin(\pi x)/(\pi x)$  and  $n_\varsigma(i, k)$  is the sampling clock frequency offset caused by additional noise with variance

$$\text{Var}[n_\varsigma] \approx \frac{\pi^2}{3} (n\varsigma)^2 \quad (1.11)$$

when  $n\varsigma \ll 1$ ,  $n_\varsigma(i, k)$  can usually be neglected. The sampling clock frequency error can cause symbol timing drift.

## 1.2 Cell Search and Synchronization

In the 3GPP LTE systems, the user equipment (UE) achieves time and frequency synchronization with a cell and detects its cell identity in the procedure of cell search. There are two kinds of cell search: initial cell search is performed when a UE is switched on or when a UE loses its synchronization; neighbor cell search must be performed periodically during idle and active modes to update the cell to be connected and to find a candidate cell for handover. A two-step hierarchical neighbor cell search process has been applied in the 3GPP LTE systems [?]. In this thesis a non-coherent detection is performed for both PSS and SSS detection.

Firstly, the primary synchronization signal (PSS) is detected in time domain to get the slot synchronization and sector identity (one among three sectors). Secondly, frame synchronization and cell group identity (one among 168 groups) are obtained by detecting the secondary synchronization signal (SSS) in frequency domain. In addition to detecting symbol timing and physical layer ID (or sector-ID) from PSS in time domain, fractional frequency offset is also estimated from PSS by making use of CP based correlation approach [?]. In general, coherent detection is usually utilized for SSS detection, where the channel response is estimated from primary synchronization channel (PSCH) by the detected PSS [?]-[?]. However, owing to the limited number of PSS, there may be more than one neighbor cell with the same PSS, and the channel response estimated from PSCH could not exactly match the channel response of the target cell. Moreover, the channel response differences between PSCH and secondary synchronization channel (SSCH) will become obvious in high Doppler frequency environment. Even in low Doppler frequency environment, in TDD mode, performance degradation is occurred by difference of channel between PSS and SSS, since PSS and SSS signals are separated by two OFDM symbols in TDD mode. To solve this problem a non-coherent detection approach for SSS detection is followed in this thesis, which has stable performance regardless of doppler frequency. In addition to detecting radio frame timing and cell-ID, integer frequency offset is also estimated using SSS signal in frequency domain. After cell search and correcting for synchronization errors, channel estimation is performed on PSS and SSS data that include both simulated data and real time captured data, using 1D-MMSE and subsequent plots are generated.

Once UE detects the cell-ID and obtains downlink synchronization of the serving cell (enodeB), UE needs to indicate its presence to the serving cell and also get up-link synchronized with the serving cell. The propagation delay encountered by each

user for transmissions between eNodeB and UE is distance dependent. Different location of UE in the cell causes unequal propagation delays, leading to misalignment of symbols at the eNodeB, which may result in loss of uplink intra-cell orthogonality. Thus eNodeB needs to estimate propagation delays of different UE's and correspondingly adjust their transmission time instant so that all the UE's gets uplink synchronized with eNodeB. After initial cell search the UE decodes the information sent on the Physical Broadcast Channel (PBCH), which includes cell specific information like Bandwidth, number of transmit antennas used by eNodeB etc. PBCH information also includes parameters required by the UE to perform uplink synchronization, which is initiated by UE by transmitting preamble to eNodeB on Physical Random Access Channel (PRACH). In this thesis both full frequency domain and hybrid time-frequency domain approach has been followed for PRACH preamble detection at eNodeB.

This thesis is organized as follows. Chapter 2 describes about PSS and SSS signals structure and generation along with the system model and frame structures in LTE. Chapter 3 describes sector and cell search along with detecting cell-ID and estimating symbol timing and frequency offsets based on proposed scheme. In Chapter 4 PRACH structure is discussed whereas in Chapter 5 practical implementation of PRACH and its detection based on proposed method are discussed. Simulation results along with the results obtained by working on real time RF captured data are presented in chapter 6. Finally conclusion and future work is presented in chapter 7.

# Chapter 2

## Downlink Synchronization signals

A UE wishing to access an LTE cell must first undertake a cell search procedure. This consists of a series of synchronization stages by which the UE determines time and frequency parameters that are necessary to demodulate the downlink and to transmit uplink signals with the correct timing. The UE also acquires some critical system parameters. Two major synchronization requirements can be identified in the LTE system: the first is symbol timing acquisition, by which the correct symbol start position is determined, for example to set the FFT window position; the second is carrier frequency synchronization, which is required to reduce or eliminate the effect of frequency errors arising from a mismatch of the local oscillators between the transmitter and the receiver, as well as the Doppler shift caused by the UE motion.

Two relevant cell search procedures exist in LTE: the first is Initial synchronization, where by the UE detects an LTE cell and decodes all the information required to register to it. This would be required, for example, when the UE is switched on, or when it has lost the connection to the serving cell; the second is the New cell identification, performed when a UE is already connected to an LTE cell and is in the process of detecting a new neighbour cell. In this case, the UE reports to the serving cell measurements related to the new cell, in preparation for handover. In both scenarios, the synchronization procedure makes use of two specially designed physical signals which are broadcast in each cell: the Primary Synchronization Signal (PSS) and the Secondary Synchronization Signal (SSS). The detection of these two signals not only enables time and frequency synchronization, but also provides the UE with the physical layer identity of the cell and the cyclic prefix length, and informs the UE whether the cell uses Frequency Division Duplex (FDD) or Time Division Duplex (TDD).

In the case of the initial synchronization, in addition to the detection of synchro-

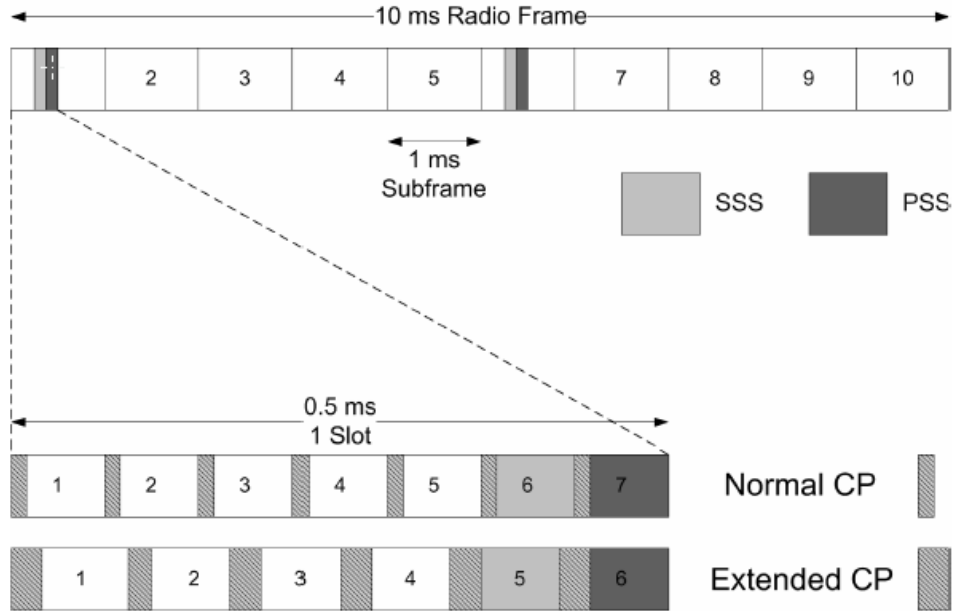


Figure 2.1: PSS and SSS frame and slot structure in time domain in the FDD case.

nization signals, the UE proceeds to decode the Physical Broadcast Channel (PBCH), from which critical system information is obtained. In the case of new cell identification, the UE does not need to decode the PBCH; it simply makes quality-level measurements based on the reference signals transmitted from the newly-detected cell and reports these to the serving cell.

The PSS and SSS structure in time is shown in Figure 2.1 for the FDD case and in Figure 2.2 for TDD: the synchronization signals are transmitted periodically, twice per 10 ms radio frame [?]. In an FDD cell, the PSS is always located in the last OFDM (Orthogonal Frequency Division Multiplexing) symbol of the first and 11<sup>th</sup> slots of each radio frame, thus enabling UE to acquire the slot boundary timing independently of the Cyclic Prefix (CP) length. The SSS is located in the symbol immediately preceding the PSS, a design choice enabling coherent detection of the SSS relative to the PSS, based on the assumption that the channel coherence duration is significantly longer than one OFDM symbol. In a TDD cell, the PSS is located in the third symbol of the 3<sup>rd</sup> and 13<sup>th</sup> slots, while the SSS is located three symbols earlier; coherent detection can be used under the assumption that the channel coherence time is significantly longer than four OFDM symbols.

In the frequency domain, the mapping of the PSS and SSS to subcarriers is shown in Figure 2.3. The PSS and SSS are transmitted in the central six Resource Blocks (RBs), enabling the frequency mapping of the synchronization signals to be invariant

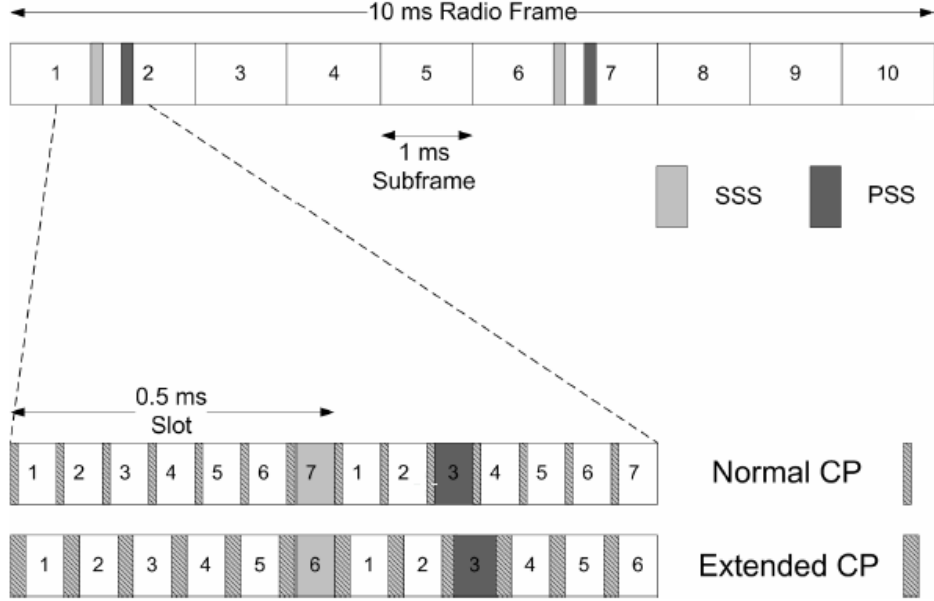


Figure 2.2: PSS and SSS frame and slot structure in time domain in the TDD case.

with respect to the system bandwidth (which can vary from 6 to 110 RBs) ; this allows the UE to synchronize to the network without any a priori knowledge of the allocated bandwidth. The PSS and SSS are each comprised of a sequence of length 62 symbols, mapped to the central 62 subcarriers around the d.c. subcarrier which is left unused. This means that the five resource elements at each extremity of each synchronization sequence are not used.

The particular sequences which are transmitted for the PSS and SSS in a given cell are used to indicate the physical-layer cell identity to the UE. There are 504 unique physical-layer cell identities. The physical-layer cell identities are grouped into 168 unique physical-layer cell-identity groups, each group containing three unique identities. The grouping is such that each physical-layer cell identity is part of one and only one physical-layer cell-identity group. A physical-layer cell identity  $N_{ID}^{cell} = 3N_{ID}^{(1)} + N_{ID}^{(2)}$  is thus uniquely defined by a number  $N_{ID}^{(1)}$  in the range of 0 to 167, representing the physical-layer cell-identity group, and a number  $N_{ID}^{(2)}$  in the range of 0 to 2, representing the physical-layer identity within the physical-layer cell-identity group. The three identities in a group would usually be assigned to cells under the control of the same eNodeB. Three PSS sequences are used to indicate the cell identity within the group, and 168 SSS sequences are used to indicate the identity of the group.



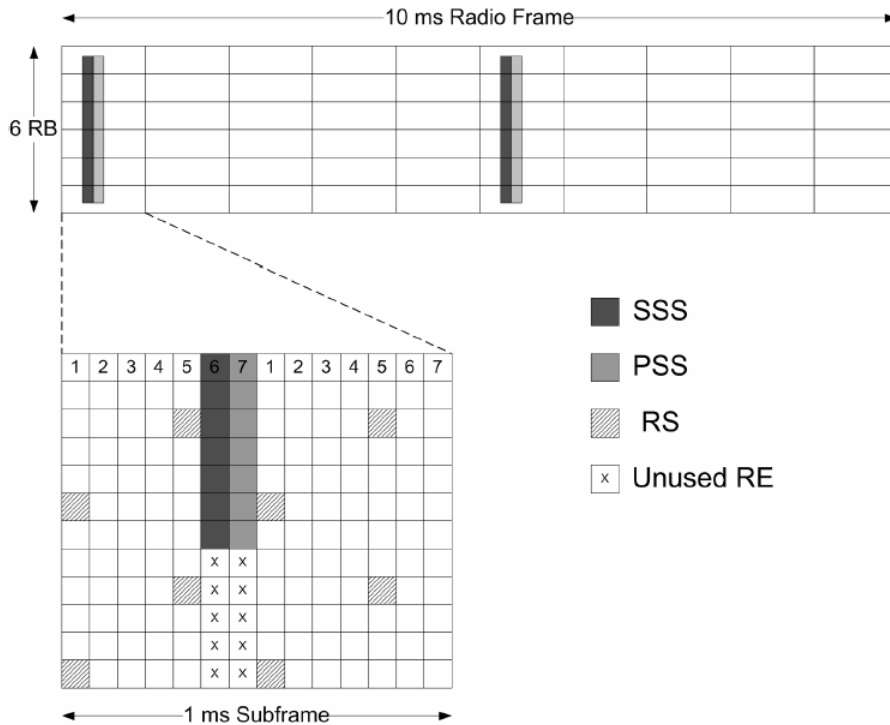


Figure 2.3: PSS and SSS frame structure in frequency and time domain for an FDD cell.

## 2.1 Primary synchronization Signal

Primary synchronization signal is constructed from one of the three length-63 Zadoff-Chu sequence in the frequency domain, with the middle element punctured to avoid transmitting on d.c subcarrier. Three PSS sequences are used in LTE, corresponding to the three physical layer identities ( $N_{ID}^{(2)} = 0, 1, 2$ ) within each group of cells.

### 2.1.1 Sequence generation

The sequence  $d(n)$  used for the primary synchronization signal is generated from a frequency-domain Zadoff-Chu sequence according to

$$d_u(n) = e^{-j\frac{un(n+1)}{63}}, \quad n = 0, 1, \dots, 62. \quad (2.1)$$

where the Zadoff-Chu root sequence index  $u$  is given by Table 3.1

This set of roots for the ZC sequences was chosen for its good periodic auto-correlation and cross-correlation properties. In particular, these sequences have a low-frequency offset sensitivity, defined as the ratio of the maximum undesired auto-correlation peak in the time domain to the desired correlation peak computed at a

$N_{ID}^{(2)}$	Root index $u$
0	25
1	29
2	34

Table 2.1: Root indices for the primary synchronization signal.

certain frequency offset. This allows a certain robustness of the PSS detection during the initial synchronization.

## 2.2 Secondary synchronization signal

The SSS consists of a frequency domain sequence, which is an interleaved concatenation of two length-31  $m$ -sequences, named as even sequence and odd sequence here. Both even sequence and odd sequence are scrambled by an  $m$ -sequence whose cyclic shift value is dependent on sector identity. The odd sequence is further scrambled by an  $m$ -sequence with cyclic shift value determined by even sequence. The combination of cyclic shifts of even sequence and odd sequence corresponds to the cell group identity. These two length-31 sequences differ every 5ms, which allows UE to detect the 10ms frame timing.

### 2.2.1 Sequence generation

The sequence  $d(0), \dots, d(61)$  used for the second synchronization signal is an interleaved concatenation of two length-31 binary sequences. The concatenated sequence is scrambled with a scrambling sequence given by the primary synchronization signal. The combination of two length-31 sequences defining the secondary synchronization signal differs between subframe 0 and subframe 5 according to

$$d(2n) = \begin{cases} s_0^{(m_0)}(n)c_0(n) & \text{in subframe 0} \\ s_1^{(m_1)}(n)c_0(n) & \text{in subframe 5} \end{cases} \quad (2.2)$$

$$d(2n+1) = \begin{cases} s_1^{(m_1)}(n)c_1(n)z_1^{(m_0)}(n) & \text{in subframe 0} \\ s_0^{(m_0)}(n)c_1(n)z_1^{(m_1)}(n) & \text{in subframe 5} \end{cases} \quad (2.3)$$

where  $0 \leq n \leq 30$ . The indices  $m_0$  and  $m_1$  are derived from the physical-layer cell-identity group  $N_{ID}^{(1)}$  according to

$$m_0 = m' \bmod 31 \quad (2.4)$$

$$m_1 = (m_0 + \lfloor m'/31 \rfloor + 1) \bmod 31 \quad (2.5)$$

$$m' = N_{ID}^{(1)} + q(q+1)/2, \quad q = \left\lfloor \frac{N_{ID}^{(1)} + q'(q'+1)/2}{30} \right\rfloor, \quad q' = \lfloor N_{ID}^{(1)}/30 \rfloor \quad (2.6)$$

where the output of the above expression is listed in Table 2.2. The two sequences  $s_0^{(m_0)}(n)$  and  $s_1^{(m_1)}(n)$  are defined as two different cyclic shifts of the  $m$ -sequence  $\tilde{s}(n)$  according to

$$s_0^{(m_0)}(n) = \tilde{s}((n + m_0) \bmod 31) \quad (2.7)$$

$$s_1^{(m_1)}(n) = \tilde{s}((n + m_1) \bmod 31) \quad (2.8)$$

where  $\tilde{s}(i) = 1 - 2x(i)$ ,  $0 \leq i \leq 30$ , is defined by

$$x(\bar{i} + 5) = (x(\bar{i} + 2) + x(\bar{i})) \bmod 2, \quad 0 \leq \bar{i} \leq 25 \quad (2.9)$$

with initial conditions  $x(0) = 0$ ,  $x(1) = 0$ ,  $x(2) = 0$ ,  $x(3) = 0$ ,  $x(4) = 1$ . The two scrambling sequences  $c_0(n)$  and  $c_1(n)$  depend on the primary synchronization signal and are defined by two different cyclic shifts of the  $m$ -sequence  $\tilde{c}(n)$  according to

$$c_0(n) = \tilde{c}((n + N_{ID}^{(2)}) \bmod 31) \quad (2.10)$$

$$c_1(n) = \tilde{c}((n + N_{ID}^{(2)} + 3) \bmod 31) \quad (2.11)$$

where  $N_{ID}^{(2)} \in \{0, 1, 2\}$  is the physical-layer identity within the physical-layer cell identity group  $N_{ID}^{(1)}$  and  $\tilde{c}(n) = 1 - 2x(n)$ ,  $0 \leq n \leq 30$ , is defined by

$$x(\bar{i} + 5) = (x(\bar{i} + 3) + x(\bar{i})) \bmod 2, \quad 0 \leq \bar{i} \leq 25$$

with initial conditions  $x(0) = 0$ ,  $x(1) = 0$ ,  $x(2) = 0$ ,  $x(3) = 0$ ,  $x(4) = 1$ .

The scrambling sequences  $z_1^{(m_0)}(n)$  and  $z_1^{(m_1)}(n)$  are defined by a cyclic shift of the  $m$ -sequence  $\tilde{z}(n)$  according to

$$z_1^{(m_0)}(n) = \tilde{z}((n + (m_0 \bmod 8)) \bmod 31) \quad (2.12)$$

$$z_1^{(m_1)}(n) = \tilde{z}((n + (m_1 \bmod 8)) \bmod 31) \quad (2.13)$$

where  $m_0$  and  $m_1$  are obtained from Table 2.2 and  $\tilde{z}(i) = 1 - 2x(i)$ ,  $0 \leq i \leq 30$ , is defined by

$$x(\bar{i} + 5) = (x(\bar{i} + 4) + x(\bar{i} + 2) + x(\bar{i} + 1) + x(\bar{i})) \bmod 2, \quad 0 \leq \bar{i} \leq 25$$

with initial conditions  $x(0) = 0$ ,  $x(1) = 0$ ,  $x(2) = 0$ ,  $x(3) = 0$ ,  $x(4) = 1$ .

$N_{ID}^{(1)}$	$m_0$	$m_1$	$N_{ID}^{(1)}$	$m_0$	$m_1$	$N_{ID}^{(1)}$	$m_0$	$m_1$	$N_{ID}^{(1)}$	$m_0$	$m_1$	$N_{ID}^{(1)}$	$m_0$	$m_1$
0	0	1	34	4	6	68	9	12	102	15	19	136	22	27
1	1	2	35	5	7	69	10	13	103	16	20	137	23	28
2	2	3	36	6	8	70	11	14	104	17	21	138	24	29
3	3	4	37	7	9	71	12	15	105	18	22	139	25	30
4	4	5	38	8	10	72	13	16	106	19	23	140	0	6
5	5	6	39	9	11	73	14	17	107	20	24	141	1	7
6	6	7	40	10	12	74	15	18	108	21	25	142	2	8
7	7	8	41	11	13	75	16	19	109	22	26	143	3	9
8	8	9	42	12	14	76	17	20	110	23	27	144	4	10
9	9	10	43	13	15	77	18	21	111	24	28	145	5	11
10	10	11	44	14	16	78	19	22	112	25	29	146	6	12
11	11	12	45	15	17	79	20	23	113	26	30	147	7	13
12	12	13	46	16	18	80	21	24	114	0	5	148	8	14
13	13	14	47	17	19	81	22	25	115	1	6	149	9	15
14	14	15	48	18	20	82	23	26	116	2	7	150	10	16
15	15	16	49	19	21	83	24	27	117	3	8	151	11	17
16	16	17	50	20	22	84	25	28	118	4	9	152	12	18
17	17	18	51	21	23	85	26	29	119	5	10	153	13	19
18	18	19	52	22	24	86	27	30	120	6	11	154	14	20
19	19	20	53	23	25	87	0	4	121	7	12	155	15	21
20	20	21	54	24	26	88	1	5	122	8	13	156	16	22
21	21	22	55	25	27	89	2	6	123	9	14	157	17	23
22	22	23	56	26	28	90	3	7	124	10	15	158	18	24
23	23	24	57	27	29	91	4	8	125	11	16	159	19	25
24	24	25	58	28	30	92	5	9	126	12	17	160	20	26
25	25	26	59	0	3	93	6	10	127	13	18	161	21	27
26	26	27	60	1	4	94	7	11	128	14	19	162	22	28
27	27	28	61	2	5	95	8	12	129	15	20	163	23	29
28	28	29	62	3	6	96	9	13	130	16	21	164	24	30
29	29	30	63	4	7	97	10	14	131	17	22	165	0	7
30	0	2	64	5	8	98	11	15	132	18	23	166	1	8
31	1	3	65	6	9	99	12	16	133	19	24	167	2	9
32	2	4	66	7	10	100	13	17	134	20	25	-	-	-
33	3	5	67	8	11	101	14	18	135	21	26	-	-	-

Table 2.2: Mapping between physical-layer cell-identity group  $N_{ID}^{(1)}$  and the indices  $m_0$  and  $m_1$

# Chapter 3

## Decoding downlink synchronization signal

### 3.1 System model

We consider the transmission of a serial discrete baseband OFDM stream  $s(n)$  given by

$$s(n) = \frac{1}{\sqrt{N}} \sum_{k=0}^{N-1} X_k e^{j2\pi kn/N}, \quad 1 \leq n \leq N \quad (3.1)$$

where  $X_k$  denotes the modulated data on the  $k$ th sub-carrier and  $N$  the FFT size. Transmitting over a multipath propagation channel under consideration of a frequency misalignment between transmitter and receiver oscillators as well as additive white Gaussian noise (AWGN), the received signal will be

$$r(n) = [s(n) \otimes h(n)] e^{j2\pi\epsilon n/N} + w(n), \quad (3.2)$$

where  $h(n)$  represents channel impulse response (CIR),  $\epsilon$  denotes the frequency mismatch with respect to the sub-carrier spacing,  $w(n)$  is the noise term and  $\otimes$  stands for circular convolution. The CIR is modeled as

$$h(n) = \sum_{d=0}^{N_d-1} h_d \delta(n-d) \quad (3.3)$$

where  $N_d$  is the number of channel taps and  $h_d$  the complex value of the  $d$ -th Rayleigh-distributed tap. The mean power of  $h_d$  follows an exponential decay and is given by

$$\sigma_d^2 = e^{-\frac{d}{\tau}}, \quad (3.4)$$

where  $\tau$  is the power decay constant.

After applying the  $N$ -point FFT at the receiver and assuming perfect timing, the OFDM symbol is given by

$$Y_l = \frac{1}{\sqrt{N}} \sum_{n=0}^{N-1} r(n) e^{-j2\pi ln/N} = \frac{1}{N} \sum_{k=0}^{N-1} H_k X_k \sum_{n=0}^{N-1} e^{2\pi(k-l+\epsilon)/N} + W_k \quad (3.5)$$

with

$$H_k = \sum_{l=0}^{N-1} h_l e^{-j2\pi kl/N} \text{ and } W_k = \frac{1}{\sqrt{N}} \sum_{n=0}^{N-1} w(n) e^{-j2\pi nk/N} \quad (3.6)$$

As it can be observed from Equation (4.5), the received OFDM symbol will be affected not only by the channel and noise distortions  $H_k$  and  $W_k$ , but also by a term due to CFO( $\epsilon$ ). The received OFDM symbol  $Y_l$  constellation will be rotated by an equal phase known as the common phase error(CPE), which is independent of the particular sub-carrier. Furthermore, the loss of orthogonality between sub-carrier has a noise-like effect called inter-carrier-interference(ICI).

## 3.2 Time and frequency synchronization

The objective of synchronization is to retrieve OFDM symbol timing and to estimate the carrier frequency offset (CFO). The CFO can be separated into an integer part, which is a multiple of the sub-carrier spacing, and a fractional part, which is responsible for the CPE and ICI. The CFO regarding the sub-carrier spacing can be thus given as

$$\epsilon = n_I + \epsilon_F,$$

where  $n_I$  is the integer number of sub-carrier spacing and  $\epsilon_F$  the fractional part with  $-1 < \epsilon < 1$ . In [?] we investigated several approaches on time and frequency synchronization for LTE. According to conclusions of this study, we decide to use the cyclic prefix based method for acquisition of the OFDM symbol timing and fractional CFO, as it is originally proposed in [?]. The log-likelihood function for the OFDM symbol start ( $\theta$ ) and the frequency mismatch ( $\epsilon_F$ ) can be written as

$$\Lambda(\theta, \epsilon_F) = 2 |\gamma(\theta)| \cos \{2\pi\epsilon_F + \angle\gamma(\theta)\} - \rho\epsilon(\theta) \quad (3.7)$$

In Equation (??) ,  $\angle$  denotes the argument of the complex number

$$\gamma(n) = \sum_{k=n}^{n+L-1} r(k)r^*(k+N) \quad (3.8)$$

is the correlation term and

$$\epsilon(n) = \sum_{k=n}^{n+L-1} |r(k)|^2 + |r(k+N)|^2 \quad (3.9)$$

the energy term, while  $L$  denotes the CP length, measured in time samples. The magnitude of the correlation coefficient between  $r(k)$  and  $r(k+N)$  is given by  $\rho \equiv \frac{\sigma_s}{\sigma_s + \sigma_n}$  , where  $\sigma_s$  and  $\sigma_n$  denote the signal and noise power respectively. The maximum likelihood( $ML$ ) estimate of  $\theta$  and  $\epsilon_F$  maximizes the function  $\Lambda(\theta, \epsilon_F)$  , and is given by

$$\hat{\theta}_{ML} = \theta \{2 |\gamma(\theta)| - \rho\epsilon(\theta)\} \quad (3.10)$$

$$\hat{\epsilon}_{F,ML} = -\frac{1}{2\pi} \angle\gamma(\hat{\theta}_{ML}) \quad (3.11)$$

The cyclic prefix based method remains unaffected by the presence of high CFO, but estimates only the fractional part  $\epsilon_F$  . Furthermore, it indicates only the OFDM symbol timing, but not the beginning of the radio frame (BOF). The performance of this method can be significantly improved by averaging  $\Lambda(\theta, \epsilon_F)$  over several OFDM symbols

## 3.3 Sector and cell search

### 3.3.1 Sector search

In order to identify the physical-layer identity or so called sector-ID( $N_{ID}^{(2)}$ ) with the highest signal level we perform a non-coherent correlation of the received symbols with replicas of the three PSS signals in the time domain according to



$$Q_i(n) = \sum_{k=0}^{N-1} d_i^*(k)r(n+k), \quad (3.12)$$

where  $d_i(k)$  denotes the replica of  $i^{\text{th}}$  PSS sequence,  $N$  is the PSS time domain signal length,  $k$  is the time domain index and  $r(k)$  the received symbols. The magnitude of the non-coherent correlator output  $|Q_i(n)|$  corresponding to the sector with the highest signal shows a large peak compared to the other correlation terms due to orthogonality between sequences. Thus, the estimated physical-layer identity or sector-ID ( $N_{ID}^{(2)}$ ) is given by

$$\hat{N}_s = \arg \max_i (|Q_i(n)|) \quad (3.13)$$

Simultaneously, the approximate position of the start of the PSS sequence from the received signal is given by

$$\hat{m}_{\hat{N}_s} = \arg \max_n (|Q_{\hat{N}_s}(n)|) \quad (3.14)$$

The maximum likelihood (ML) estimate of the start of the PSS symbol and also the fractional frequency offset can be found out by Cyclic prefix correlation based on Equations (??) and (??) respectively. Simultaneously, the sector identification indicates the radio frame start as the PSS sequence position within the radio frame is already known, however with an uncertainty between first and sixth sub-frame. This information is retrieved by decoding the SSS signal, as explained in following Section (??)

### 3.4 Cell-ID search and Integer carrier frequency offset estimation

The cell-ID needs to be estimated correctly, in order to establish connection with the best possible serving base station. The group-ID  $N_{ID}^{(1)}$  can be jointly estimated with the integer Carrier Frequency Offset (CFO)  $n_I$  and the sub-frame index within the radio frame (0 or 5). The basic concept is to exploit the cyclic shifts of the two length-31 binary sequences  $s_0^{(m_0)}(n)$  and  $s_1^{(m_1)}(n)$  according to the pair of integers  $m_0$  and  $m_1$ , which identify the group-ID. The quantity of integer CFO  $n_I$  can be estimated by the sub-carrier shift of the frequency domain SSS sequence  $d(n)$ . The method proposed here consists of following steps:

- Extract the SSS signal according to the estimated OFDM symbol timing and apply an  $N$ -point FFT.
- Separate 62 length sequence  $d(n)$  into sequence  $d(2n)$  and  $d(2n + 1)$ , consisting of even and odd sub-carrier symbols  
*In the following we use the notation of sub-frame 0:*
- Divide  $d(2n)/c_0(n)$  in order to obtain the sequence  $s_0^{(m_0)}(n)$ . Sequence  $c_0(n)$  is known at the receiver as it depends only on the already estimated sector-ID  $N_{ID}^{(2)}$ .
- Build a reference sequence  $s_{ref}(n)$ , which is a duplicated version of  $s_0^{(m_0=0)}$  or  $s_1^{(m_1=0)}$  with the length of 62
- Apply a cross-correlation between  $s_0^{(m_0)}(n)$  and the reference sequence  $s_{ref}(n)$ . The magnitude of the correlation term shows a significant maximum location which indicates the estimate of  $m_0$
- After estimating the integer  $m_0$ , we are able to compute  $z_1^{(m_0)}(n)$  which is obtained by cyclically shifting already known reference sequence  $z_1(n)$  by the estimated integer  $m_0$  and afterwards divide  $d(2n + 1)/(c_1(n)z_1^{(m_0)}(n))$  in order to obtain the sequence  $s_1^{(m_1)}(n)$ .
- Apply a cross-correlation between  $s_1^{(m_1)}(n)$  and  $s_{ref}(n)$ . The magnitude of the correlation term shows a significant maximum at a position, which is estimated as integer  $m_1$ .
- The pair of estimated  $m_0$  and  $m_1$  identifies the group-ID  $N_{ID}^{(1)}$
- Compute the overall cell-ID :  $N_{ID}^{cell} = 3N_{ID}^{(1)} + N_{ID}^{(2)}$

The described procedure is performed for several cyclic shifts of  $d(n)$  (where the cyclic shifts are varied for instance from -15 to +15 sub-carriers), in order to detect the integer CFO part  $n_I$ . Significant peaks will only be generated if the received sequence  $d(n)$  is compensated for the integer CFO  $n_I$ . The cyclic shift of  $d(n)$  for which significant peaks occurs gives the estimated integer CFO.

# Chapter 4

## Uplink Synchronizations

Random access channel is an uplink channel which acts as an interface between non-synchronized UE's and the orthogonal transmission scheme of the LTE uplink radio access, unless and until a UE is uplink synchronized any uplink transmission is not possible. Physical Random Access Channel (PRACH) is the physical layer equivalent of a Random access channel (RACH), i.e it defines the time-frequency resource on which RACH preamble is actually transmitted.

### 4.1 Initial access

Before the user equipment can start transmitting and receiving data it must connect to the network. This connection phase consists of 3 stages where UE (Terminal) extracts some set of information in each stage. The three stages that each UE should undergo before any transmission or reception are given below. This combined process is known as LTE initial access

#### 4.1.1 Cell search

The first thing that happens in the access procedure is that the UE gets identified within the network. This procedure is called the cell search, which includes in establishment of synchronization between UE and the cell and acquiring the information about cell. The synchronization procedures are performed in order to obtain timing synchronization for correct symbol detection and also for frequency synchronization to annihilate frequency mismatches caused by movement of UE or different oscillators at the receiving and transmitting sides. The downlink synchronization is achieved by receiving primary and secondary synchronization sequences, details of which are

explained in chapter 2 and 3.

### **4.1.2 Derive system information**

The second part of the access procedure is where the UE needs to derive system information. This system information is periodically broadcasted in the network and this information is needed for the UE to be able to connect to the network and a specific cell within that network. When the UE has received and decoded the system information it has information about for example cell bandwidths and parameters specific to random access.

### **4.1.3 Random access**

Random access is used to achieve uplink time synchronization for a UE which either has not yet acquired, or has lost its uplink synchronization. Once uplink synchronization is achieved for a UE, the eNodeB can schedule orthogonal uplink transmission resources for it. Random access is generally performed when the UE turns on from sleep mode, performs handoff from one cell to another or when it loses uplink timing synchronization. Random access allows the eNodeB to estimate and, if needed, adjust the UE uplink transmission timing to within a fraction of the cyclic prefix. When an eNodeB successfully receives a random access preamble, it sends a random access response indicating the successfully received preamble(s) along with the timing advance (TA) and uplink resource allocation information to the UE. The UE can then check if its random access attempt has been successful by matching the preamble number it used for random access with the preamble number information received from the eNodeB. If the preamble number matches, the UE concludes that its preamble transmission attempt has been successful and it then adjust its uplink timing based on the Timing Advance(T.A) that it has received. If the preamble number does not match then it tries for retransmission. After the UE has acquired uplink timing synchronization, it can transmit data in uplink.

### **4.1.4 Timing correction**

The propagation delay encountered by each user for transmissions between eNodeB and UE is distance dependent i.e, user very close to base station encounters less

delay compared to cell edge user. If suppose the near by user and cell edge user are allocated with same uplink time resource but different frequency resources (Resource blocks) then because of unequal propagation delays in their transmissions on uplink the reception of both users at eNodeB may not be aligned properly which may result in loss of uplink intra-cell orthogonality, in contrary if both users are allocated with same frequency resource but different time instants there is every possibility that the transmission of one user may get smeared into the transmission of next user (with an assumption that preceding user is cell edge user) which may lead to inter symbol interference.

In order to avoid timing misalignment of different users at eNodeB, if eNodeB could be able to calculate their propagation delays a priori by some means and instruct each user to correct its timing before transmission of any data on uplink then all UE transmissions can be perfectly aligned at eNodeB. The Random access process helps eNodeB in figuring out the propagation delays of each UE, eNodeB calculates the propagation delays of all UEs from their preamble transmissions on PRACH and then instructs corresponding UE to correct its timing of transmission, i.e. either advance in time or retard in time, i.e. upon receiving this command cell edge user will advance his transmission by the amount specified by the eNodeB, i.e. if cell edge user is allotted a time slot  $t$  for its transmission and if it is instructed to advance by  $t_1$  seconds to counter its propagation delay then instead of transmitting at  $t^{th}$  interval the cell edge user starts transmitting before  $t^{th}$  i.e. at  $(t - t_1)^{th}$  instant.

## 4.2 Random Access Procedure

A downlink synchronized UE which needs to achieve uplink synchronization will transmit a random access preamble (signature) on uplink on time-frequency resources as specified by the system. Each cell comprises of 64 random access preambles and UE which requires uplink synchronization randomly selects one of the preambles and transmits it on uplink PRACH. When a UE transmits a PRACH Preamble, it transmits with a specific pattern and this specific pattern is called a "Signature".

The random access process occurs in two forms in LTE, which indicate either contention-based (possibility of collision) or contention-free. In the case of contention-based random access procedure each UE randomly selects one among the available random access preamble signatures, with a possibility for more than one UE simultaneously to transmit the same preamble signature, which needs a contention resolution procedure. On the other hand if a UE needs to perform a handover, where UE is al-

ready in connection mode, the eNodeB allocates dedicated signatures to UE from the group of signatures which are exclusively allotted for contention-free purpose. Thus the contention-free random access procedure has no possibility of collision, leading to a faster random access procedure, which is crucial in case of handover.

A cell has a fixed number 64 of preamble signatures, and these signatures are partitioned between those for contention-based access and those reserved for allocation to specific UE's on a contention-free basis. The two procedures are outlined in the following sections.

### 4.2.1 Contention-based Random Access Procedure

The contention-based procedure is a four step process, as shown in Figure ??

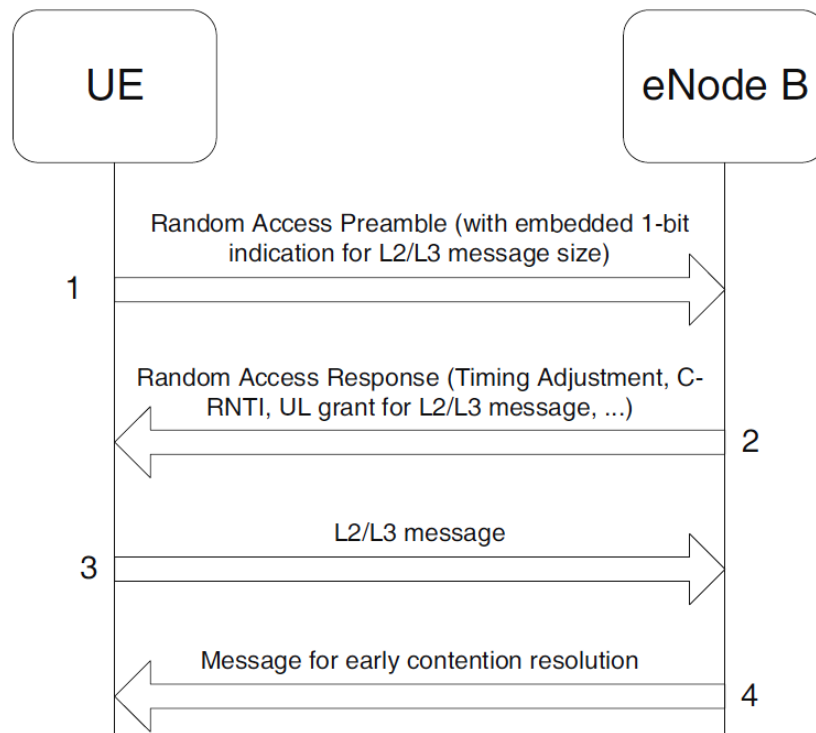


Figure 4.1: Contention-based Random Access Procedure

#### Step 1: Transmission of Random Access Preamble:

The UE randomly picks one of the contention based preamble signature and transmit it on PRACH allowing the eNodeB to estimate the transmission timing of the terminal. Preamble signatures allocated for contention-based procedure are further divided into two groups based on the size of transmission resource needed by UE

for step 3, which include small transmission resource demanding preambles and large transmission resource demanding preambles. The purpose behind this division is if suppose the message to be transmitted at step 3 is of small size and eNodeB has allotted more resources for subsequent transmission then it may lead to inefficient usage of uplink time-frequency resources. Based on transmission resource needed for transmission of data in step 3 UE selects randomly one preamble among the two subgroups of contention based preambles and transmit that preamble on the radio resources as allocated by the eNodeB. The eNodeB can control the number of preamble signatures in each group based on the observed loads. The initial preamble transmission power setting is based on an open-loop estimation with full compensation for the path-loss. This is designed to ensure that the received power of the preambles is independent of the path-loss; this is designed to help the eNodeB to detect several simultaneous preamble transmissions in the same time-frequency PRACH resource. The UE estimates the path-loss by averaging measurements of the downlink Reference Signal Received Power (RSRP). The radio resources on which RACH process should occur will be configured by eNodeB and propagated through broadcast channel as a part of system information

### **Step 2: Random access response:**

In response to the transmitted preamble, eNodeB transmits a random access response (RAR) on physical downlink shared channel which contains

- Random Access Radio Network Temporary Identifier (RA-RNTI)

- Timing alignment command
- Initial uplink resource grant for transmission of the message in step 3
- Temporary Cell Radio Network Temporary Identifier (C-RNTI).

**Random Access Radio Network Temporary Identifier (RA-RNTI)** :It identifies which time-frequency resources are utilized by the UE to transmit the Random Access Preamble i.e the time-frequency slot in which the preamble was transmitted, the RA-RNTI is essentially the sub frame number in which the UE has transmitted which gets added by 1. After UE transmits its preamble, it waits for a RAR (random access response) associated with its implicit RA-RNTI to see if the eNodeB heard the preamble. If it finds a suitable RAR, then it looks to see if its specific preamble sequence is included; if so, then the UE assumes it received a positive

acknowledge from the eNodeB and proceeds with subsequent steps.

The RA-RNTI is determined from the UE's preamble transmission; the temporary C-RNTI is assigned by the eNodeB. Any UE sending a preamble in subframe  $n$  will look for a response with an RA-RNTI with value  $n + 1$ ; it then has to parse the response to see if there's a specific RAR in the response corresponding to the preamble the UE used. Up to 64 UEs can send a preamble in the same subframe, and still be distinguished (assuming they manage to pick a unique preamble). If multiple UEs has transmitted the same preamble on same time-frequency resources all of them obviously receive the same RA-RNTI.

**Timing alignment command:** Based on the propagation delay associated with each UE transmission (measured from Transmitted preamble), the network determines the required timing correction for each UE. If the timing of a specific terminal needs correction, the network issues a timing advance command for this specific terminal, instructing it to retard or advance its timing relative to the current uplink timing, and this command is very much necessary in order to maintain synchronization among multiple UE uplink transmissions.

**Initial uplink resource grant for transmission of the message:** This specifies the amount of resource allocated by eNodeB for step 3 message transmission. It includes a 10 bit fixed size resource block, and type of modulation and coding scheme to be employed which will be indicated via a 4 bit string and transmission power control command indicated by 3 bit string, uplink delay and CQI request each indicated by one bit.

**Temporary Cell Radio Network Temporary Identifier:** TC-RNTI is a temporary identifier assigned by the eNodeB to UE by means of which UE can perform subsequent signaling to the eNodeB. C-RNTI is used by a given UE while it is in a particular cell, where the UE is already in connected mode. If no prior allotted C-RNTI is available with UE then it uses temporary RNTI for further communication between the UE and eNodeB, if communication is successful then TC-RNTI is promoted to C-RNTI.

The UE expects to receive the RAR within a time window, of which the start and end are configured by the eNodeB and broadcast as part of the cell-specific system information. The earliest subframe allowed by the specifications occurs 2 ms after the end of the preamble sub frame. However, a typical delay (measured from the



end of the preamble subframe to the beginning of the first subframe of RAR window) is more likely to be 4 ms. If the UE is unable to receive the RAR within the specified RAR slot as configured by eNodeB then the UE needs to retransmit the preamble after some backoff time and this backoff-time, which specifies the time UE need to wait after RAR window to retransmit the preamble is configured by eNodeB. Every retransmission comes with increase in transmission power, UE retransmits the preamble with slightly higher power compared to original transmission and the increase of power in each retransmission is known as power ramping and is configured by eNodeB as power-ramping-step. The UE need to stop transmitting preamble after some successive trails, the number of retransmission that UE should undergo is also configured by eNodeB.

### **Step 3: Message on UL-SCH:**

The uplink of the UE terminal will get time synchronized after receiving the RAR. However, before user data can be transmitted to/from the terminal, a unique identity within the cell, the C-RNTI, must be assigned to the terminal. Depending on the terminal (UE) state, there may also be a need for additional message exchange for setting up the connection. In the third step, the terminal transmits the necessary messages to the eNodeB using the UL-SCH resources assigned in the random-access response in the second step

Once UE receives Random access response and successfully decodes it and extracts the provided uplink grant and C-RNTI (TC-RNTI in case of initial access), UE starts transmitting the layer2/layer3 message on specified uplink resource ,this transmission may be a request for RRC connection establishment, tracking area updates or scheduling request etc. If suppose more than one user has transmitted the same preamble on same time-frequency resource in step 1 then all of those UE's receive the same RAR allocating same time-frequency resource and same TC-RNTI and all these users in contention will transmit their corresponding L2/L3 messages on same time-frequency resource which may lead to one of the two possibilities One possibility is that these multiple signals act as interference to each other and eNodeB decodes neither of them in this case, none of the UE would have any response (HARQ ACK) from eNodeB and they all think that RACH process has failed and go back to step 1. The other possibility would be that eNodeB could successfully decode the message from only one UE and failed to decode it from the other UE in this case, the UE with the successful L2/L3 decoding on eNodeB side will get the HARQ ACK from eNodeB.

#### Step 4: Contention resolution:

The Hybrid Automatic Repeat Request Acknowledgment process (HARQ) for step 3 message is called "contention resolution" process. Contention resolution message is addressed to C-RNTI (in case of RRC-Connected) or to temporary C-RNTI . Upon reception of contention resolution message any one of the three possibilities may happen at UE

- The UE correctly decodes the message and detects its own identity: it sends back a Positive Acknowledgment, ACK.
- The UE correctly decodes the message and discovers that it contains another UEs identity (contention resolution) it sends nothing back (Discontinuous Transmission,DTX).
- The UE fails to decode the message or misses the DL grant: it sends nothing back('DTX').

#### 4.2.2 Contention free random access

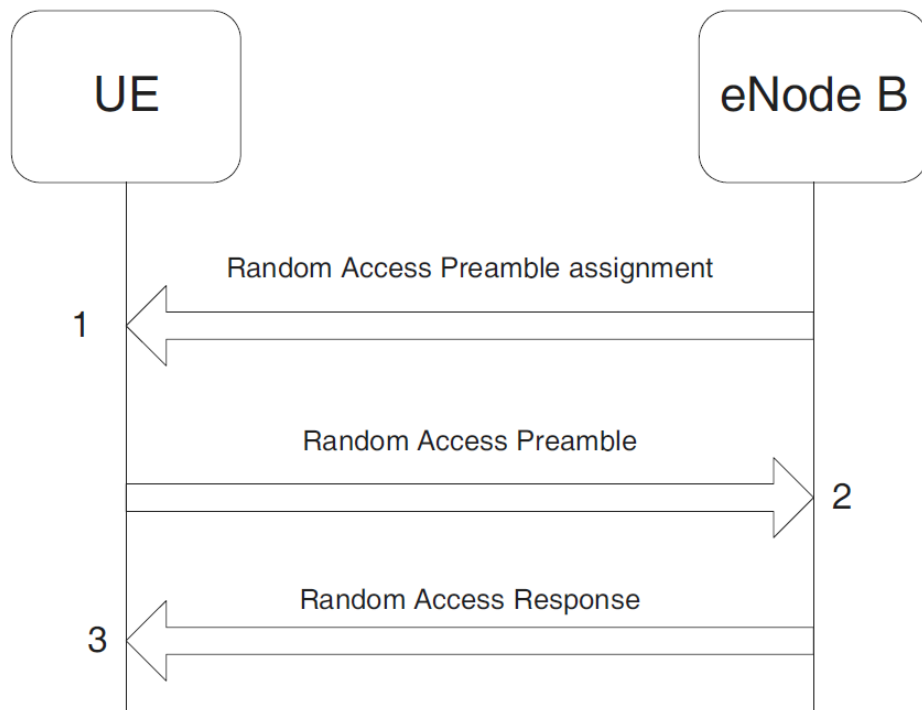


Figure 4.2: Contention-free Random Access Procedure

Each UE is assigned with a dedicated preamble signature in the case of Contention-free random access, leaving no scope for contention. This contention-free random access is extremely useful where low latency is required, such as handover and resumption of downlink traffic for a UE. Contention free random access is a two step process as shown in Figure ??

Preamble transmission and RAR are similar to that of contention based process except that a dedicated preamble is transmitted where as in contention based a randomly selected preamble was transmitted, since there is hardly any chance for contention in this process message on uplink granted resource and contention resolution steps are not required.

## 4.3 PRACH resource requirements

### 4.3.1 Time resource

The time resource allocated for preamble transmission depends on the time duration of the preamble to be transmitted, which varies with radius of cell in which UE is located. Based on radius of cell to cover four different preamble formats are defined, each having varying lengths of cyclic prefix and preamble lengths. A preamble slot in time domain consists of 3 parts, which include Preamble sequence, Cyclic prefix and Guard period. To account for the timing uncertainty and to avoid interference with subsequent subframes which are not used for Random access (may be used by PUSCH for data transmission), a guard time is used as part of the preamble transmission. Before the start of random access UE has however achieved downlink synchronization but yet to achieve uplink synchronization and hence there is a definite timing uncertainty associated with each UE's uplink transmission as the location of the terminal in the cell is not known and this uncertainty is proportional to the cell size and amounts to  $6.7\mu\text{s}/\text{km}$  and that's why a guard period is appended in PRACH slot as a part of preamble transmission. The use of cyclic prefix in PRACH preamble transmission allows for frequency domain processing at the base station and also it may even be used to absorb Inter Symbol Interference in case of large cell where delay spread may extend guard period.

The minimum time duration configured for each RACH slot is 1ms. RACH transmission is actually multiplexed with physical uplink shared channel transmission (PUSCH), there is no separate resource for RACH transmission. Depending upon

the radius of cell to cover different preamble formats are configured by eNodeB for subsequent transmission on RACH, preamble formats occupies a time duration of 1ms to 3ms depending upon their preamble and cyclic-prefix lengths. The basic random access sequence is of 1ms which can be employed to cover a cell of radius less than 15 km However in order to accommodate the cyclic prefix and guard time the actual preamble sequence is shortened and is less than 1ms.

### 4.3.2 Sequence duration

The length of preamble sequence should be chosen with care and is driven by some factors which are listed below

- Trade-off between sequence length and overhead: A single sequence must be as long as possible to maximize the number of orthogonal preambles while still fitting within a single subframe in order to keep the PRACH overhead small in most deployments, i.e. selected sequence should be such that the cyclic shifts of sequence which results in other orthogonal preambles should account for total preamble sequences available with cell(64);
- Compatibility with the maximum expected round-trip delay;
- Compatibility between PRACH and PUSCH subcarrier spacings;
- Coverage performance

**Constraint 1:** The sequence length,  $T_{seq}$  should be more than  $683.33\mu s$ .

Since the purpose of preamble transmission is to achieve uplink synchronization, which includes estimation of propagation delay of user uplink transmission and issuing an appropriate timing correction command, and hence length of preamble sequence should account for round-trip time delay for a UE located at the edge of the largest expected cell (100 km radius), including the maximum delay spread expected in such large cells (Typically  $16.67\mu s$ ).

$$T_{seq} \geq ((100 \times 2 \times 10^3)/(3 \times 10^8)) + (16.67 \times 10^{-6})s = 683.33\mu s.$$

**Constraint 2:** The length of preamble sequence should be integer multiple of normal OFDM symbol duration (because PUSCH transmission is based on OFDM) Since RACH transmission is multiplexed with PUSCH transmission it is desirable to minimize the orthogonality loss in the frequency domain between the preamble subcarriers and the subcarriers of the surrounding uplink data transmissions on PUSCH. This is achieved if the PUSCH data symbol subcarrier spacing  $\Delta f$  is an integer mul-

tuple of the PRACH subcarrier spacing  $\Delta f_{RA}$ :

$$T_{SEQ} = k \times T_{SYM} = k/\Delta f, \quad k \in N$$

**Constraint 3:** The maximum length of a preamble sequence (preamble format 0 and 1) should not exceed  $813\mu s$ . The potential coverage performance of a 1 ms PRACH preamble is in the region of 14 kms as a consequence, the required CP and GT lengths are approximately  $14 \times 10^3 / (3 \times 10^8) = 93.5\mu s$ . As we know that preamble transmission should accommodate CP and GT and hence maximum length of sequence should be  $1000 - (2 \times 93.5) = 813\mu s$ . By considering the three constraints stated above the ideal length of the sequence that satisfies all these three constraints is  $T_{seq} = 800\mu s$  for preamble format 0 and 1. Depending on the duration of the sequence and also the duration of CP (cyclic prefix), GT (guard time) four different formats are present:

Preamble format	Number of allocated subframes	CP duration ( $\mu s$ )	GT duration ( $\mu s$ )	Max.delay spread ( $\mu s$ )	Max.cell radius (km)
0	1	103.13	96.88	6.25	14.53
1	2	684.38	515.63	16.67	77.34
2	2	203.13	196.88	6.25	29.53
3	3	684.38	715.63	16.67	100.16

Table 4.1: Preamble formats

### 4.3.3 Frequency resource

Frequency resource of 6 Resource Blocks(RB's) which turns out to 1.08 Mhz is assigned for PRACH transmission irrespective of the system bandwidth. In order to maintain the orthogonality between the data subcarriers (transmitted on PUSCH) and RACH subcarriers, the spacing of PRACH subcarriers is chosen with care, two constraints should be considered before subcarrier spacing selection:

- 1) It (spacing) should result in orthogonality among the PRACH sub carriers.
- 2) It should provide orthogonality between PRACH and PUSCH transmission.

In order to preserve orthogonality, the PUSCH subcarrier spacing (15Khz) should be integer multiple of PRACH sub carrier spacing . The ideal subcarrier spacing which meet the above two requirements is  $\Delta f_{RA} = 1, 25$  kHz. This subcarrier spacing is quite different from normal subcarrier spacing. The optimal length of Preamble in time do-

main is  $800\mu s$  and corresponding length in frequency domain is  $1080/1.25 = 864$  sub carriers.

## 4.4 Resource allocation for PRACH

The resource allocated for PRACH will be different for FDD mode and TDD mode. The following section describes the frame structure in LTE and PRACH resource allocation for Frame structure type1 (applicable for FDD) and Frame structure type2 (applicable for TDD).

Downlink and uplink transmissions are organized into radio frames with  $T_f = 307200 \times T_s = 10ms$  duration, where  $T_s = 1/(15000 \times 2048)s$  is the sampling time duration. Two radio frame structure are supported in LTE, described in the following sections

### 4.4.1 PRACH resources for frame structure type 1:

Each radio frame defined in LTE is  $T_f = 307200 \times T_s = 10ms$  long and consists of 20 slots of length  $T_{slot} = 15360 \times T_s = 0.5ms$ , numbered from 0 to 19. Each subframe consists of two consecutive slots. In case of FDD 10 subframes are available for downlink transmission and 10 subframes are available for uplink transmissions in each 10 ms interval. Uplink and downlink transmissions are separated in the frequency domain. In half-duplex FDD operation, the UE cannot transmit and receive at the same time while there are no such restrictions in full-duplex FDD.

For frame structure type 1 with preamble format 0 – 3, there is at most one random access resource per subframe. Table-?? lists the Frame structure type 1 random access configuration for preamble format 0 – 3 and the subframes in which random access preamble transmission is allowed for a given configuration in frame structure type 1. The parameter PRACH-ConfigurationIndex is given by higher layers. The start of the random access preamble shall be aligned with the start of the corresponding uplink subframe at the UE. For PRACH configuration 0, 1, 2, 15, 16, 17, 18, 31, 32, 33, 34, 47, 48, 49, 50 and 63 the UE may for handover purposes assume an absolute value of the relative time difference between radio frame  $i$  in the current cell and the target cell of less than  $153600 \times T_s$ . The first physical resource block  $n_{PRB}^{RB}$  allocated to the PRACH opportunity considered for preamble format 0, 1, 2 and 3 is defined as  $n_{PRB}^{RB} = n_{PRBoffset}^{RB}$ , where the parameter PRACH-FrequencyOffset  $n_{PRBoffset}^{RB}$  is expressed as a physical resource block number configured by higher layers and fulfilling

$0 \leq n_{PRBoffset}^{RB} \leq N_{UL}^{RB} - 6$ , where the parameter  $N_{UL}^{RB}$  represents number of resource blocks allocated for uplink.

PRACH Configuration Index	Preamble Format	System frame number	Subframe number
0	0	Even	1
1	0	Even	4
2	0	Even	7
3	0	Any	1
4	0	Any	4
5	0	Any	7
6	0	Any	1, 6
7	0	Any	2, 7
8	0	Any	3, 8
9	0	Any	1, 4, 7
10	0	Any	2, 5, 8
11	0	Any	3, 6, 9
12	0	Any	0, 2, 4, 6, 8
13	0	Any	1, 3, 5, 7, 9
14	0	Any	0, 1, 2, 3, 4, 5, 6, 7, 8, 9
15	0	Even	9
16	1	Even	1
17	1	Even	4
18	1	Even	7
19	1	Any	1
20	1	Any	4
21	1	Any	7
22	1	Any	1, 6
23	1	Any	2, 7
24	1	Any	3, 8
25	1	Any	1, 4, 7
26	1	Any	2, 5, 8
27	1	Any	3, 6, 9
28	1	Any	0, 2, 4, 6, 8
29	1	Any	1, 3, 5, 7, 9
30	N/A	N/A	N/A
31	1	Even	9
32	2	Even	1
33	2	Even	4
34	2	Even	7
35	2	Any	1



PRACH Configuration Index	Preamble Format	System frame number	Subframe number
36	2	Any	4
37	2	Any	7
38	2	Any	1, 6
39	2	Any	2, 7
40	2	Any	3, 8
41	2	Any	1, 4, 7
42	2	Any	2, 5, 8
43	2	Any	3, 6, 9
44	2	Any	0, 2, 4, 6, 8
45	2	Any	1, 3, 5, 7, 9
46	N/A	N/A	N/A
47	2	Even	9
48	3	Even	1
49	3	Even	4
50	3	Even	7
51	3	Any	1
52	3	Any	4
53	3	Any	7
54	3	Any	1, 6
55	3	Any	2, 7
56	3	Any	3, 8
57	3	Any	1, 4, 7
58	3	Any	2, 5, 8
59	3	Any	3, 6, 9
61	N/A	N/A	N/A
62	N/A	N/A	N/A
63	3	Even	9

Table 4.2: : Frame structure type 1 random access configuration for preamble format 0-3

#### 4.4.2 PRACH resources for frame structure type 2:

Frame structure type 2 is applicable to TDD. Each radio frame of length  $T_f = 307200 \times T_s = 10ms$  consists of two half-frames of length  $153600 \times T_s = 5ms$  each. Each half-frame consists of five subframes of length  $30720 \times T_s = 1ms$ . The supported uplink-downlink configurations are listed in Table-?? where, for each subframe in a radio frame, D denotes the subframe is reserved for downlink transmissions, U denotes the subframe is reserved for uplink transmissions and S denotes a special subframe with the three fields DwPTS, GP and UpPTS as shown in Figure ???. The total

length of DwPTS, GP and UpPTS being equal to  $30720 \times T_s = 1\text{ms}$ . Each subframe  $i$  is defined as two slots,  $2i$  and  $2i + 1$  of length  $T_{slot} = 15360 \times T_s = 0.5\text{ms}$  in each subframe.

Uplink-downlink configurations with both 5 ms and 10 ms downlink-to-uplink switch-point periodicity are supported. In case of 5 ms downlink-to-uplink switch-point periodicity, the special subframe exists in both half-frames. In case of 10 ms downlink-to-uplink switch-point periodicity, the special subframe exists in the first half-frame only. Subframes 0 and 5 and DwPTS are always reserved for downlink transmission. UpPTS and the subframe immediately following the special subframe are always reserved for uplink transmission.

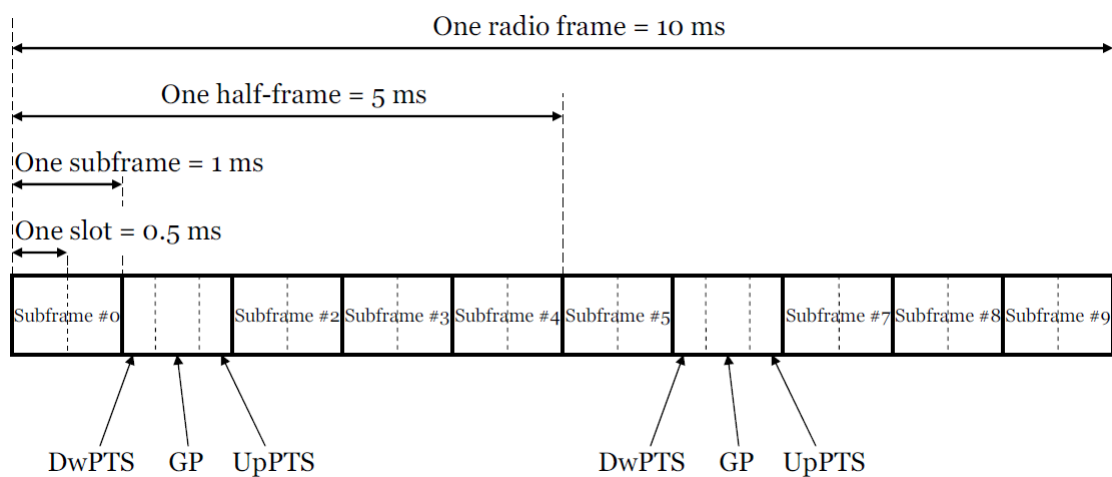


Figure 4.3: Frame structure Type 2

Uplink-downlink configuration	Downlink-to-Uplink Switch-point periodicity	Subframe number									
		0	1	2	3	4	5	6	7	8	9
0	5 ms	D	S	U	U	U	D	S	U	U	U
1	5 ms	D	S	U	U	D	D	S	U	U	D
2	5 ms	D	S	U	D	D	D	S	U	D	D
3	10 ms	D	S	U	U	U	D	D	D	D	D
4	10 ms	D	S	U	U	D	D	D	D	D	D
5	10 ms	D	S	U	D	D	D	D	D	D	D
6	5 ms	D	S	U	U	U	D	S	U	U	D

Table 4.3: Uplink-Downlink Configuration Type 2

For frame structure type 2 with preamble format 0 – 4, there might be multiple random access resources in an UL subframe (or UpPTS for preamble format 4) depending on the UL/DL configuration, as shown in Table-??. Table-?? lists the mapping to physical resources for the different random access opportunities needed for corresponding PRACH Configuration-index, which is assigned by higher layers. Each quadruple of the format  $(f_{RA}, t_{RA}^0, t_{RA}^1, t_{RA}^2)$  indicates the location of a specific random access resource, where  $f_{RA}$  is a frequency resource index within the considered time instance,  $t_{RA}^2 = 0, 1, 2$  indicates whether the resource is reoccurring in all radio frames, in even radio frames, or in odd radio frames, respectively,  $t_{RA}^1 = 0, 1$  indicates whether the random access resource is located in first half frame or in second half frame, respectively, and where  $t_{RA}^2$  is the uplink subframe number where the preamble starts, counting from 0 at the first uplink subframe between 2 consecutive downlink-to-uplink switch points, with the exception of preamble format 4 where  $t_{RA}^2$  is denoted as (\*). The start of the random access preamble formats 0 – 3 shall be aligned with the start of the corresponding uplink subframe at the UE assuming  $N_{TA} = 0$ , and the random access preamble format 4 shall start  $4832 \times T_s$  before the end of the UpPTS at the UE, where the UpPTS is referenced to the UEs uplink frame timing assuming  $N_{TA} = 0$ , where  $N_{TA} = 0$  is the timing offset between uplink and downlink radio frames at the UE, expressed in units of  $T_s$ . The random access opportunities for each PRACH configuration shall be allocated in time first and then in frequency if and only if time multiplexing is not sufficient to hold all opportunities of a PRACH configuration. For preamble format 0 – 3, the frequency multiplexing

shall be done according to

$$n_{PRB}^{RA} = \begin{cases} n_{PRB\ offset}^{RA} + 6 \lfloor \frac{f_{RA}}{2} \rfloor, & \text{if } f_{RA} \bmod 2 = 0 \\ N_{RB}^{UL} - 6 - n_{PRB\ offset}^{RA} - 6 \lfloor \frac{f_{RA}}{2} \rfloor, & \text{otherwise} \end{cases} \quad (4.1)$$

where  $N_{RB}^{UL}$  is the number of uplink resource blocks  $n_{PRB}^{RB}$  is the first physical resource block allocated to the PRACH opportunity considered and where the parameter prach-FrequencyOffset  $n_{PRB\ offset}^{RB}$  is the first physical resource block available for PRACH expressed as a physical resource block number configured by higher layers and fulfilling  $0 \leq n_{PRB\ offset}^{RB} \leq N_{RB}^{UL} - 6$ .

For preamble format 4, the frequency multiplexing shall be done according to

$$n_{PRB}^{RA} = \begin{cases} 6f_{RA}, & \text{if } ((n_f \bmod 2) \times (2 - N_{SP}) + t_{RA}^1) \bmod 2 = 0 \\ N_{RB}^{UL} - 6(f_{RA} + 1), & \text{otherwise} \end{cases} \quad (4.2)$$

where  $n_f$  is the system frame number and where  $N_{SP}$  is the number of DL to UL switch points within the radio frame. Each random access preamble occupies a bandwidth corresponding to 6 consecutive resource blocks for both frame structure.

PRACH configuration Index	UL/DL configuration						
	0	1	2	3	4	5	6
0	(0,1,0,2)	(0,1,0,1)	(0,1,0,0)	(0,1,0,2)	(0,1,0,1)	(0,1,0,0)	(0,1,0,2)
1	(0,2,0,2)	(0,2,0,1)	(0,2,0,0)	(0,2,0,2)	(0,2,0,1)	(0,2,0,0)	(0,2,0,2)
2	(0,1,1,2)	(0,1,1,1)	(0,1,1,0)	(0,1,0,1)	(0,1,0,0)	N/A	(0,1,1,1)
3	(0,0,0,2)	(0,0,0,1)	(0,0,0,0)	(0,0,0,2)	(0,0,0,1)	(0,0,0,0)	(0,0,0,2)
4	(0,0,1,2)	(0,0,1,1)	(0,0,1,0)	(0,0,0,1)	(0,0,0,0)	N/A	(0,0,1,1)
5	(0,0,0,1)	(0,0,0,0)	N/A	(0,0,0,0)	N/A	N/A	(0,0,0,1)
6	(0,0,0,2)	(0,0,0,1)	(0,0,0,0)	(0,0,0,1)	(0,0,0,0)	(0,0,0,0)	(0,0,0,2)
	(0,0,1,2)	(0,0,1,1)	(0,0,1,0)	(0,0,0,2)	(0,0,0,1)	(1,0,0,0)	(0,0,1,1)
7	(0,0,0,1)	(0,0,0,0)	N/A	(0,0,0,0)	N/A	N/A	(0,0,0,1)
	(0,0,1,1)	(0,0,1,0)	(0,0,0,2)	(0,0,0,2)			(0,0,1,0)
8	(0,0,0,0)	N/A	N/A	(0,0,0,0)	N/A	N/A	(0,0,0,0)
	(0,0,1,0)			(0,0,0,1)			(0,0,1,1)
9	(0,0,0,1)	(0,0,0,0)	(0,0,0,0)	(0,0,0,0)	(0,0,0,0)	(0,0,0,0)	(0,0,0,1)
	(0,0,0,2)	(0,0,0,1)	(0,0,1,0)	(0,0,0,1)	(0,0,0,1)	(1,0,0,0)	(0,0,0,2)
	(0,0,1,2)	(0,0,1,1)	(1,0,0,0)	(0,0,0,2)	(1,0,0,1)	(2,0,0,0)	(0,0,1,1)
10	(0,0,0,0)	(0,0,0,1)	(0,0,0,0)	N/A	(0,0,0,0)	N/A	(0,0,0,0)
	(0,0,1,0)	(0,0,1,0)	(0,0,1,0)		(0,0,0,1)		(0,0,0,2)
	(0,0,1,1)	(0,0,1,1)	(1,0,1,0)		(1,0,0,0)		(0,0,1,0)
11	N/A	(0,0,0,0)	N/A	N/A	N/A	N/A	(0,0,0,1)
		(0,0,0,1)					(0,0,1,0)
		(0,0,1,0)					(0,0,1,1)
12	(0,0,0,1)	(0,0,0,0)	(0,0,0,0)	(0,0,0,0)	(0,0,0,0)	(0,0,0,0)	(0,0,0,1)
	(0,0,0,2)	(0,0,0,1)	(0,0,1,0)	(0,0,0,1)	(0,0,0,1)	(1,0,0,0)	(0,0,0,2)
	(0,0,1,1)	(0,0,1,0)	(1,0,0,0)	(0,0,0,2)	(1,0,0,0)	(2,0,0,0)	(0,0,1,0)
	(0,0,1,2)	(0,0,1,1)	(1,0,1,0)	(1,0,0,2)	(1,0,0,1)	(3,0,0,0)	(0,0,1,1)
13	(0,0,0,0)	N/A	N/A	(0,0,0,0)	N/A	N/A	(0,0,0,0)
	(0,0,0,2)			(0,0,0,1)			(0,0,0,1)
	(0,0,1,0)			(0,0,0,2)			(0,0,0,2)
	(0,0,1,2)			(1,0,0,1)			(0,0,1,1)
14	(0,0,0,0)	N/A	N/A	(0,0,0,0)	N/A	N/A	(0,0,0,0)
	(0,0,0,1)			(0,0,0,1)			(0,0,0,2)
	(0,0,1,0)			(0,0,0,2)			(0,0,1,0)
	(0,0,1,1)			(1,0,0,0)			(0,0,1,1)
15	(0,0,0,0)	(0,0,0,0)	(0,0,0,0)	(0,0,0,0)	(0,0,0,0)	(0,0,0,0)	(0,0,0,0)
	(0,0,0,1)	(0,0,0,1)	(0,0,1,0)	(0,0,0,1)	(0,0,0,1)	(1,0,0,0)	(0,0,0,1)
	(0,0,0,2)	(0,0,1,0)	(1,0,0,0)	(0,0,0,2)	(1,0,0,0)	(2,0,0,0)	(0,0,0,2)
	(0,0,1,1)	(0,0,1,1)	(1,0,1,0)	(1,0,0,1)	(1,0,0,1)	(3,0,0,0)	(0,0,1,0)
	(0,0,1,2)	(1,0,0,1)	(2,0,0,0)	(1,0,0,2)	(2,0,0,1)	(4,0,0,0)	(0,0,1,1)
16	(0,0,0,1)	(0,0,0,0)	(0,0,0,0)	(0,0,0,0)	(0,0,0,0)	N/A	N/A
	(0,0,0,2)	(0,0,0,1)	(0,0,1,0)	(0,0,0,1)	(0,0,0,1)		
	(0,0,1,0)	(0,0,1,0)	(1,0,0,0)	(0,0,0,2)	(1,0,0,0)		
	(0,0,1,1)	(0,0,1,1)	(1,0,1,0)	(1,0,0,0)	(1,0,0,1)		
	(0,0,1,2)	(1,0,1,1)	(2,0,1,0)	(1,0,0,2)	(2,0,0,0)		
17	(0,0,0,0)	(0,0,0,0)	N/A	(0,0,0,0)	N/A	N/A	N/A
	(0,0,0,1)	(0,0,0,1)		(0,0,0,1)			
	(0,0,0,2)	(0,0,1,0)		(0,0,0,2)			
	(0,0,1,0)	(0,0,1,1)		(1,0,0,0)			
	(0,0,1,2)	(1,0,0,0)		(1,0,0,1)			
18	(0,0,0,0)	(0,0,0,0)	(0,0,0,0)	(0,0,0,0)	(0,0,0,0)	(0,0,0,0)	(0,0,0,0)
	(0,0,0,1)	(0,0,0,1)	(0,0,1,0)	(0,0,0,1)	(0,0,0,1)	(1,0,0,0)	(0,0,0,1)
	(0,0,0,2)	(0,0,1,0)	(1,0,0,0)	(0,0,0,2)	(1,0,0,0)	(2,0,0,0)	(0,0,0,2)
	(0,0,1,0)	(0,0,1,1)	(1,0,1,0)	(1,0,0,0)	(1,0,0,1)	(3,0,0,0)	(0,0,1,0)
	(0,0,1,1)	(1,0,0,1)	(2,0,0,0)	(1,0,0,1)	(2,0,0,0)	(4,0,0,0)	(0,0,1,1)
	(0,0,1,2)	(1,0,1,1)	(2,0,1,0)	(1,0,0,2)	(2,0,0,1)	(5,0,0,0)	(1,0,0,2)
19	N/A	(0,0,0,0)	N/A	N/A	N/A	N/A	(0,0,0,0)
		(0,0,0,1)					(0,0,0,1)
		(0,0,1,0)					(0,0,0,2)
		(0,0,1,1)					(0,0,1,0)
		(1,0,0,0)					(0,0,1,1)
		(1,0,1,0)					(1,0,1,1)
20 / 30	(0,1,0,1)	(0,1,0,0)	N/A	(0,1,0,1)	(0,1,0,0)	N/A	(0,1,0,1)
21 / 31	(0,2,0,1)	(0,2,0,0)	N/A	(0,2,0,1)	(0,2,0,0)	N/A	(0,2,0,1)
22 / 32	(0,1,1,1)	(0,1,1,0)	N/A	N/A	N/A	N/A	(0,1,1,0)
23 / 33	(0,0,0,1)	(0,0,0,0)	N/A	(0,0,0,1)	(0,0,0,0)	N/A	(0,0,0,1)
24 / 34	(0,0,1,1)	(0,0,1,0)	N/A	N/A	N/A	N/A	(0,0,1,0)

PRACH configuration Index	UL/DL configuration						
	0	1	2	3	4	5	6
25 / 35	(0,0,0,1) (0,0,1,1)	(0,0,0,0) (0,0,1,0)	N/A	(0,0,0,1) (1,0,0,1)	(0,0,0,0) (1,0,0,0)	N/A	(0,0,0,1) (0,0,1,0)
26 / 36	(0,0,0,1) (0,0,1,1) (1,0,0,1)	(0,0,0,0) (0,0,1,0) (1,0,0,0)	N/A	(0,0,0,1) (1,0,0,1) (2,0,0,1)	(0,0,0,0) (1,0,0,0) (2,0,0,0)	N/A	(0,0,0,1) (0,0,1,0) (1,0,0,1)
27 / 37	(0,0,0,1) (0,0,1,1) (1,0,0,1) (1,0,1,1)	(0,0,0,0) (0,0,1,0) (1,0,0,0) (1,0,1,0)	N/A	(0,0,0,1) (1,0,0,1) (2,0,0,1) (3,0,0,1)	(0,0,0,0) (1,0,0,0) (2,0,0,0) (3,0,0,0)	N/A	(0,0,0,1) (0,0,1,0) (1,0,0,1) (1,0,1,0)
28 / 38	(0,0,0,1) (0,0,1,1) (1,0,0,1) (1,0,1,1) (2,0,0,1)	(0,0,0,0) (0,0,1,0) (1,0,0,0) (1,0,1,0) (2,0,0,0)	N/A	(0,0,0,1) (1,0,0,1) (2,0,0,1) (3,0,0,1) (4,0,0,1)	(0,0,0,0) (1,0,0,0) (2,0,0,0) (3,0,0,0) (4,0,0,0)	N/A	(0,0,0,1) (0,0,1,0) (1,0,0,1) (1,0,1,0) (2,0,0,1)
29 / 39	(0,0,0,1) (0,0,1,1) (1,0,0,1) (1,0,1,1) (2,0,0,1) (2,0,1,1)	(0,0,0,0) (0,0,1,0) (1,0,0,0) (1,0,1,0) (2,0,0,0) (2,0,1,0)	N/A	(0,0,0,1) (1,0,0,1) (2,0,0,1) (3,0,0,1) (4,0,0,1) (5,0,0,1)	(0,0,0,0) (1,0,0,0) (2,0,0,0) (3,0,0,0) (4,0,0,0) (5,0,0,0)	N/A	(0,0,0,1) (0,0,1,0) (1,0,0,1) (1,0,1,0) (2,0,0,1) (2,0,1,0)
40	(0,1,0,0)	N/A	N/A	(0,1,0,0)	N/A	N/A	(0,1,0,0)
41	(0,2,0,0)	N/A	N/A	(0,2,0,0)	N/A	N/A	(0,2,0,0)
42	(0,1,1,0)	N/A	N/A	N/A	N/A	N/A	N/A
43	(0,0,0,0)	N/A	N/A	(0,0,0,0)	N/A	N/A	(0,0,0,0)
44	(0,0,1,0)	N/A	N/A	N/A	N/A	N/A	N/A
45	(0,0,0,0) (0,0,1,0)	N/A	N/A	(0,0,0,0) (1,0,0,0)	N/A	N/A	(0,0,0,0) (1,0,0,0)
46	(0,0,0,0) (0,0,1,0) (1,0,0,0)	N/A	N/A	(0,0,0,0) (1,0,0,0) (2,0,0,0)	N/A	N/A	(0,0,0,0) (1,0,0,0) (2,0,0,0)
47	(0,0,0,0) (0,0,1,0) (1,0,0,0) (1,0,1,0)	N/A	N/A	(0,0,0,0) (1,0,0,0) (2,0,0,0) (3,0,0,0)	N/A	N/A	(0,0,0,0) (1,0,0,0) (2,0,0,0) (3,0,0,0)
48	(0,1,0,*)	(0,1,0,*)	(0,1,0,*)	(0,1,0,*)	(0,1,0,*)	(0,1,0,*)	(0,1,0,*)
49	(0,2,0,*)	(0,2,0,*)	(0,2,0,*)	(0,2,0,*)	(0,2,0,*)	(0,2,0,*)	(0,2,0,*)
50	(0,1,1,*)	(0,1,1,*)	(0,1,1,*)	N/A	N/A	N/A	(0,1,1,*)
51	(0,0,0,*)	(0,0,0,*)	(0,0,0,*)	(0,0,0,*)	(0,0,0,*)	(0,0,0,*)	(0,0,0,*)
52	(0,0,1,*)	(0,0,1,*)	(0,0,1,*)	N/A	N/A	N/A	(0,0,1,*)
53	(0,0,0,*) (0,0,1,*)	(0,0,0,*) (0,0,1,*)	(0,0,0,*) (0,0,1,*)	(0,0,0,*) (1,0,0,*)	(0,0,0,*) (1,0,0,*)	(0,0,0,*) (1,0,0,*)	(0,0,0,*) (0,0,1,*)
54	(0,0,0,*) (0,0,1,*) (1,0,0,*)	(0,0,0,*) (0,0,1,*) (1,0,0,*)	(0,0,0,*) (0,0,1,*) (1,0,0,*)	(0,0,0,*) (1,0,0,*) (2,0,0,*)	(0,0,0,*) (1,0,0,*) (2,0,0,*)	(0,0,0,*) (1,0,0,*) (2,0,0,*)	(0,0,0,*) (0,0,1,*) (1,0,0,*)
55	(0,0,0,*) (0,0,1,*) (1,0,0,*) (1,0,1,*)	(0,0,0,*) (0,0,1,*) (1,0,0,*) (1,0,1,*)	(0,0,0,*) (0,0,1,*) (1,0,0,*) (1,0,1,*)	(0,0,0,*) (1,0,0,*) (2,0,0,*) (3,0,0,*)	(0,0,0,*) (1,0,0,*) (2,0,0,*) (3,0,0,*)	(0,0,0,*) (1,0,0,*) (2,0,0,*) (3,0,0,*)	(0,0,0,*) (0,0,1,*) (1,0,0,*) (1,0,1,*)
56	(0,0,0,*) (0,0,1,*) (1,0,0,*) (1,0,1,*) (2,0,0,*)	(0,0,0,*) (0,0,1,*) (1,0,0,*) (1,0,1,*) (2,0,0,*)	(0,0,0,*) (0,0,1,*) (1,0,0,*) (1,0,1,*) (2,0,0,*)	(0,0,0,*) (1,0,0,*) (2,0,0,*) (3,0,0,*) (4,0,0,*)	(0,0,0,*) (1,0,0,*) (2,0,0,*) (3,0,0,*) (4,0,0,*)	(0,0,0,*) (1,0,0,*) (2,0,0,*) (3,0,0,*) (4,0,0,*)	(0,0,0,*) (0,0,1,*) (1,0,0,*) (1,0,1,*) (2,0,0,*)
57	(0,0,0,*) (0,0,1,*) (1,0,0,*) (1,0,1,*) (2,0,0,*) (2,0,1,*)	(0,0,0,*) (0,0,1,*) (1,0,0,*) (1,0,1,*) (2,0,0,*) (2,0,1,*)	(0,0,0,*) (0,0,1,*) (1,0,0,*) (1,0,1,*) (2,0,0,*) (2,0,1,*)	(0,0,0,*) (1,0,0,*) (2,0,0,*) (3,0,0,*) (4,0,0,*) (5,0,0,*)	(0,0,0,*) (1,0,0,*) (2,0,0,*) (3,0,0,*) (4,0,0,*) (5,0,0,*)	(0,0,0,*) (1,0,0,*) (2,0,0,*) (3,0,0,*) (4,0,0,*) (5,0,0,*)	(0,0,0,*) (0,0,1,*) (1,0,0,*) (1,0,1,*) (2,0,0,*) (2,0,1,*)
58	N/A	N/A	N/A	N/A	N/A	N/A	N/A
59	N/A	N/A	N/A	N/A	N/A	N/A	N/A
60	N/A	N/A	N/A	N/A	N/A	N/A	N/A
61	N/A	N/A	N/A	N/A	N/A	N/A	N/A
62	N/A	N/A	N/A	N/A	N/A	N/A	N/A
63	N/A	N/A	N/A	N/A	N/A	N/A	N/A

Table 4.4: Frame structure type2

## 4.5 Preamble sequence design

In Random access process multiple users may be transmitting randomly chosen preambles on same time-frequency resources, and hence all these preambles from multiple users must be orthogonal to each other or else it may lead to serious interference among these transmitted preambles leading to failure of random access process. The sequence that is to be transmitted as a preamble should be appropriately chosen such that it should be able to provide orthogonality among different transmitted preambles and also the selected sequence should minimize the overhead on PRACH transmission and it should meet the power requirements.

Considering the above constraints laid on the preamble sequence, a special sequence termed as prime-length ZadoffChu (ZC) sequences have been chosen to generate the preamble sequence. ZC sequences are non-binary unit-amplitude sequences, which satisfy a Constant Amplitude Zero Autocorrelation (CAZAC) property. The ZC sequence of odd-length  $N_{ZC}$  is given by

$$x_u(n) = e^{-j2\pi u \frac{n(n+1)+ln}{N_{ZC}}} \quad (4.3)$$

Where  $u = \{0, 1, \dots, N_{ZC}\}$  is the ZC sequence root index

$n = \{0, 1, 2, \dots, N_{ZC}\}$

$l = \text{any integer}$ . But in LTE we take  $l=0$  for simplicity.

Pseudo-Noise (PN) based sequences were used in WCDMA (wide band CDMA) for random access process, in LTE prime-length ZadoffChu (ZC) sequences are used. Zadoff-chu sequence comes with many attractive properties; three among them which are very much important in dealing with synchronization and minimizing interference is given below

- A ZC sequence has a constant amplitude and also its  $N_{ZC}$  point DFT also has a constant amplitude. This property limits the Peak-to-Average Ratio and generates bounded and time-flat interference to other users
- ZC sequences of any length have ideal cyclic autocorrelation (i.e. the correlation with its circularly shifted version is a delta function). The zero autocorrelation property may be formulated as:

$$r_{kk} = \sum_{n=0}^{N_{ZC}-1} x_u(n)x_u^*(n+\sigma) = \delta(\sigma) \quad (4.4)$$

where  $r_{kk}(\cdot)$  is the discrete periodic autocorrelation function of  $x_u$  at lag  $\sigma$ . This

property is of major interest when the received signal is correlated with a reference sequence and the received reference sequences are misaligned.

- The absolute value of the cyclic cross-correlation function between any two ZC sequences is constant and equal to  $1/\sqrt{N_{ZC}}$  if  $|u_1 - u_2|$  (where  $u_1$  and  $u_2$  are the sequence root indices) is relatively prime with respect to  $N_{ZC}$  (a condition that can be easily guaranteed if  $N_{ZC}$  is a prime number).

#### 4.5.1 Zadoff-Chu(ZC)sequence length

The sequence length design should address the following requirements:

- Maximize the number of ZC sequences with optimal cross-correlation properties.
- Minimize the interference to/from the surrounding scheduled data on the PUSCH.

The former requirement is guaranteed by choosing a prime-length Zadoff-chu(ZC) sequence. For the latter, since data and preamble OFDM symbols are neither aligned nor have the same durations, strict orthogonality cannot be achieved. At least, fixing the preamble duration to an integer multiple of the PUSCH symbol provides some compatibility between preamble and PUSCH subcarriers. However, with the  $800\mu\text{s}$  duration, the corresponding sequence length would be 864, which does not meet the prime number requirement for length of ZC sequence. The PRACH uses guard bands to avoid the data interference at preamble edges. In the absence of interference, there is no significant performance difference between sequences of similar prime length. In the presence of interference, it can be seen that reducing the ZC-sequence length below 839 gives no further improvement in detection rate. No effect is observed on the false alarm rate. Therefore the ZC-sequence length of 839 is selected for LTE PRACH, corresponding to 69.91 PUSCH subcarriers in each SC-FDMA symbol, and offers  $72 - 69.91 = 2.09$  PUSCH subcarriers protection, which is very close to one PUSCH subcarrier protection on each side of the preamble. So the preamble is positioned centrally in the block of 864 available PRACH subcarriers, with 12.5 null subcarriers on each side.

#### 4.5.2 Random Access cyclic shifts

Each cell needs to generate 64 different preambles from ZC-sequence of length 839 samples and all of these preambles should be orthogonal to each other so as to avoid any sort of interference among different RACH transmissions on same time-frequency resource, in such case by exploiting the cyclic auto correlation of ZC sequence if all



preambles can be generated from same root sequence then all of them will be orthonormal to each other, but it is not possible in all cases. For small cells which typically are less than 1km this may be possible but however for large cells generating all 64 signatures (all orthogonal to each other) from a single root sequence is not possible. The cyclic shift offset  $N_{CS}$  configured by eNodeB dictates the preamble generation from root sequence, it specifies with how many samples a given root sequence should cyclically shifted to ensure orthogonality among different preambles. The cyclic shift offset  $N_{CS}$  is dimensioned so that the Zero Correlation Zone (ZCZ) of the sequences guarantees the orthogonality of the PRACH sequences regardless of the delay spread and time uncertainty of the UEs. The minimum value of  $N_{CS}$  should therefore be the smallest integer number of sequence sample periods that is greater than the maximum delay spread and time uncertainty of an uplink non-synchronized UE, plus some additional guard samples provisioned for the spill-over of the pulse shaping filter envelope present in the PRACH receiver. As delay spread and timing uncertainty of large cells are high and hence  $N_{CS}$  value will also be high and with that high cyclic shift value it is not possible to generate all 64 preambles with a single root sequence and hence for large cells multiple root sequences are employed to generate all required preamble signatures. Some cell scenarios and their corresponding cyclic shift values and their coverage range are shown in Table: ??

Cell scenario	No of Cyclic shifts Per ZC sequence	No of ZC root Sequences	Cyclic Shift Size $N_{CS}$	Cell Radius In Km
1	64	1	13	0.7
2	32	2	26	2.5
3	18	4	46	2.5
4	9	8	93	12

Table 4.5: Different cell scenarios and their corresponding cyclic shifts and their typical coverage

Cyclic shift offset  $N_{CS}$  is specified by eNodeB and falls in range of 13 to 839 and hence to configure it by eNodeB, it requires to transmit 10 bit value corresponding to a particular cyclic shift as a part of system information, instead to avoid transmission of 10 bit string, all possible cyclic shift values corresponding to all formats are quantized to just 16 values. The 16 allowed values of  $N_{CS}$  were chosen so that the number of orthogonal preambles is as close as possible to what could be obtained if there were no restrictions on the value of  $N_{CS}$ . The 16 quantized set of cyclic shift offset values

and corresponding formats to be used are given in Table:??.

Cyclic prefix Offset $N_{CS}$	Format	Range in Km
13	0	0.79
15	0	1.08
18	0	1.51
22	0	2.08
26	0	2.65
32	0	3.51
38	0	4.37
46	0	5.51
59	0	7.37
76	0	9.8
93	2	12.23
119	2	15.95
167	1,3	22.82
279	1,3	38.84
419	1,3	58.86
839	1,3	118

Table 4.6: Quantized cyclic shift offset values for low speed cells

For a given cell, based on its radius a cyclic shift offset value,  $N_{CS}$  is configured by eNodeB and is transmitted via broadcast channel as a part of system information, and different cyclic shift values ( $C_v$ ) are derived from configured cyclic shift offset using the relation

$$C_v = \begin{cases} v.N_{CS} & \text{where } v = 1, 2, 3, \dots, N_{ZC}/N_{CS} \\ 0 & \text{for } N_{CS} = 0 \end{cases} \quad (4.5)$$

Once we get  $C_v$ , we can generate multiple preambles by circular shifting of the given ZC-sequence of root index  $u$  using the following function

$$x_{u,v}(n) = x_u((n + C_v) \bmod N_{ZC}) \quad (4.6)$$

### 4.5.3 Baseband prach signal generation

The time-continuous random access signal  $s(t)$  is defined by

$$s(t) = \beta_{\text{PRACH}} \sum_{k=0}^{N_{\text{ZC}}-1} \sum_{n=0}^{N_{\text{ZC}}-1} x_{u,v}(n) \cdot e^{-j\frac{2\pi nk}{N_{\text{ZC}}}} \cdot e^{j2\pi(k+\phi+K(k_0+1/2))\Delta f_{\text{RA}}(t-T_{\text{CP}})} \quad (4.7)$$

where  $0 \leq t < T_{\text{seq}} + T_{\text{CP}}$

$\beta_{\text{PRACH}}$  is an amplitude scaling factor in order to conform to the transmit power

$$k_0 = n_{\text{PRB}}^{\text{RB}} N_{\text{SC}}^{\text{RB}} - N_{\text{RB}}^{\text{UL}} N_{\text{SC}}^{\text{RB}} / 2$$

$N_{\text{RB}}^{\text{UL}}$ :The uplink system bandwidth (in RBs).

$N_{\text{SC}}^{\text{RB}}$ :The number of subcarriers per RB, i.e. 12.

$n_{\text{PRB}}^{\text{RB}}$ :It is the parameter which controls the location in the frequency domain, expressed as a resource block number configured by higher layers and fulfilling

$$0 \leq n_{\text{PRB}}^{\text{RB}} < N_{\text{RB}}^{\text{UL}} - 6$$

$K = \Delta f / \Delta f_{\text{RA}}$  accounts for the ratio of subcarrier spacing between the PUSCH and PRACH

$\phi$ : a fixed offset determining the frequency-domain location of the random access preamble within the physical resource blocks.The variable  $\Delta f_{\text{RA}}$  and  $\phi$  values for different preamble formats are given in the Table:??

Preamble format	$\Delta f_{\text{RA}}$	$\phi$
0 - 3	1250 Hz	7
4	7500 Hz	2

Table 4.7: Random access baseband parameters

# Chapter 5

## PRACH Implementation

### 5.1 UE Transmitter

At UE PRACH can be generated on the assigned time frequency resource in one of the two ways:

- Full frequency domain
- Hybrid time/frequency domain

#### 5.1.1 Full frequency domain

In this method PRACH preamble is generated just like as a normal OFDM symbol at the system sampling rate, where the samples are DFT precoded (optional) and an IDFT block preceded with subcarrier mapping is used for preamble generation, in order to support large cells the same preamble sequence is repeated to lengthen the sequence as discussed in preamble formats and a cyclic prefix is appended to ensure frequency domain processing at receiver and the same is shown in Figure:??

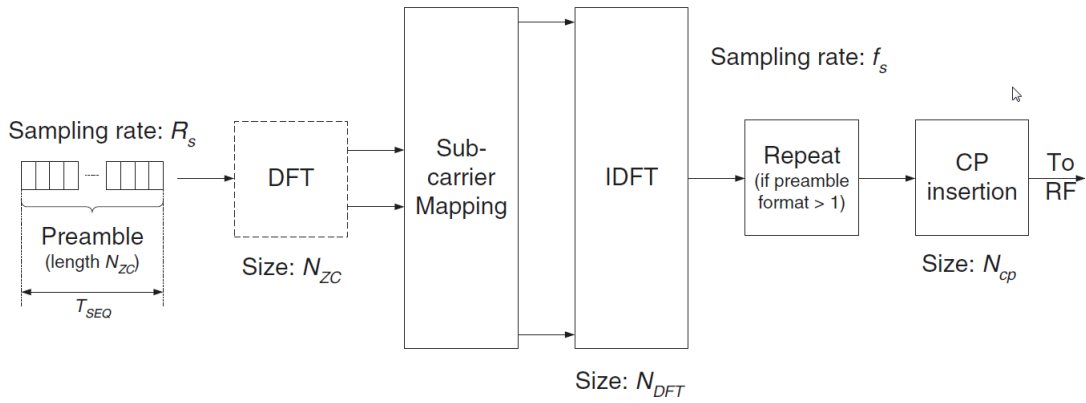


Figure 5.1: Full frequency domain PRACH transmitter

The method described above does not require any time-domain filtering at base-band, but leads to large IDFT sizes (up to 24576 for a 20 MHz spectrum allocation), which are cumbersome to implement in practice.

### 5.1.2 Hybrid time/frequency domain

The concept behind this method is to use a smaller size IFFT instead of using a very large size IDFT, and shifting the preamble to the required frequency location through time-domain upsampling and filtering, as shown in figure ?? . Given that the preamble sequence length is 839, the smallest IFFT size that can be used is 1024, resulting in a sampling frequency of  $f_{IFFT} = 1.28$  Msps. Both the CP and the sequence durations have been designed to provide an integer number of samples at this sampling rate. The CP can be inserted before the upsampling and time-domain frequency shift, so as to minimize the intermediate storage requirements.

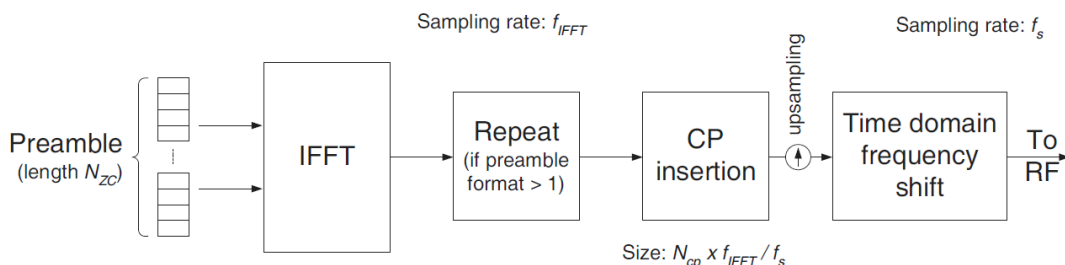


Figure 5.2: Hybrid frequency/time domain PRACH generation

## 5.2 PRACH Receiver

The receiver at the eNodeB can also be chosen between Full frequency domain and Hybrid time/Frequency domain, as shown in Figure ?? . In full frequency domain the computation of frequency tones carrying the PRACH signals is carried out directly from the received  $800\mu\text{s}$  duration signal with in observation interval, the full range of frequency tones used for uplink transmission given the system bandwidth. It does not require any time domain filtering or frequency shifts but demands for a large sized DFT.

The hybrid time/frequency-domain method first extracts the relevant PRACH signal through a time-domain frequency shift with down-sampling and anti-aliasing filtering. There follows a small-size DFT computing the set of frequency tones centered on the PRACH tones, which can then be extracted. The down-sampling ratio and corresponding anti-aliasing filter are chosen to deliver a number of PRACH time samples suitable for an FFT or simple DFT computation at a sampling rate which is an integer fraction of the system sampling rate.

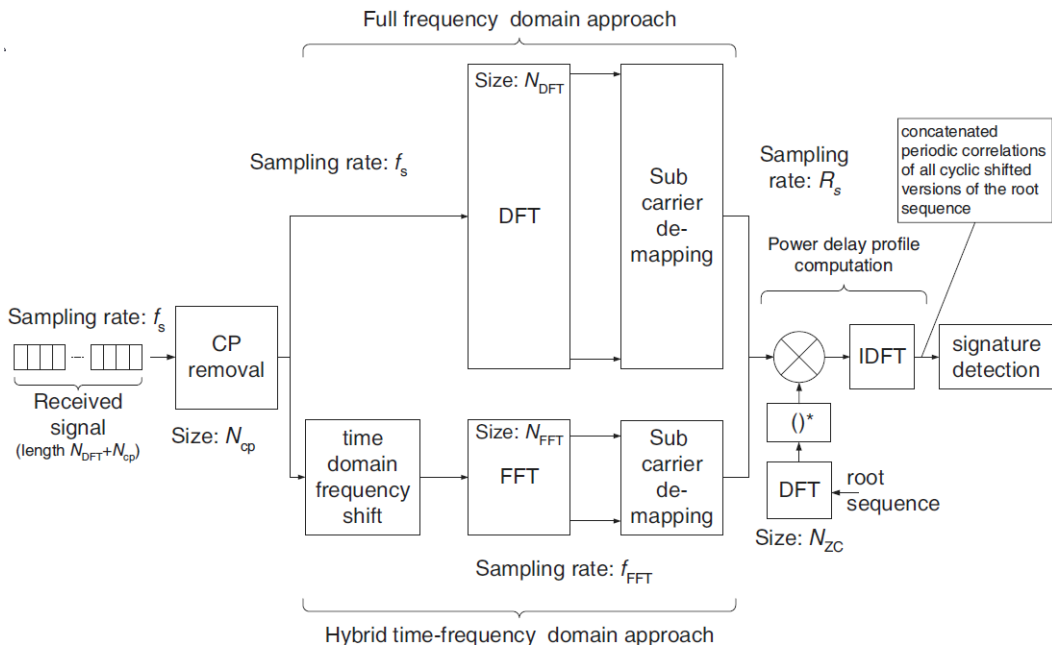


Figure 5.3: PRACH receiver

### 5.2.1 Power delay profile computation

Power delay profile of a PRACH preamble is computed as a discrete periodic correlation between received sequence  $y(n)$  and the reference searched  $N_{\text{ZC}}$  length Zadoff-chu

sequence  $x_u(n)$ .Cyclic prefix appended at transmitter ensures the frequency domain periodic correlation at receiver, and minimizes the computational complexity for PDP computation.The following section describes how to compute the PDP profile of each preamble.The discrete periodic correlation,  $z_u(l)$  at lag  $l$  between the received sequence  $y(n)$  and reference sequence  $x_u(n)$  is given as

$$|z_u(l)|^2 = \left| \sum_{n=0}^{N_{ZC}-1} y(n)x_u^*[(n+l)N_{ZC}] \right|^2 \quad (5.1)$$

$z_u(l)$  can also be expressed as follows

$$z_u(l) = [y(n) * x_u^*(-n)](l) \quad (5.2)$$

Let  $X_u(k) = R_{X_u}(k) + jI_{X_u}(k)$ ,  $Y_u(k) = R_Y(k) + jI_Y(k)$  and  $Z_u(k)$  be the DFT coefficients of the time-domain ZC sequence  $x_u(n)$ , the received baseband samples  $y(n)$ , and the discrete periodic correlation function  $z_u(n)$  respectively. Using the properties of the DFT,  $Z_u(n)$  can be efficiently computed in the frequency domain as

$$Z_u(k) = Y(K)X_u^*(k) \quad \text{for } k = 0, \dots, N_{ZC} - 1 \quad (5.3)$$

$z_u(n)$  can be computed by taking IDFT of  $Z_u(k)$  which is given as

$$z_u(n) = \sum_{k=0}^{N_{ZC}-1} Z_u(k)e^{j2\pi kn/N_{ZC}} \quad \text{for } n = 0, \dots, N_{ZC} - 1 \quad (5.4)$$

The received signal in frequency domain is complex-conjugate multiplied with frequency domain root ZC sequence. Due to the fact that frequency domain complex multiplication with root ZC sequence is equal to time domain cyclic correlation, IFFT of the multiplied sequence gives time domain cyclic correlation .

## 5.2.2 Sequence detection

The PRACH signatures which are transmitted are generated from cyclic shifts of a common root sequence means that frequency-domain computation of a root sequence provides in one shot the concatenated PDP's of all signatures derived from the same root sequence. Therefore, the signature detection process consists of searching, within each ZCZ(Zero Correlation Zone) defined by each cyclic shift, the PDP peaks above a detection threshold over a search window corresponding to the cell size. Figure:??

shows the basic function of signature detection

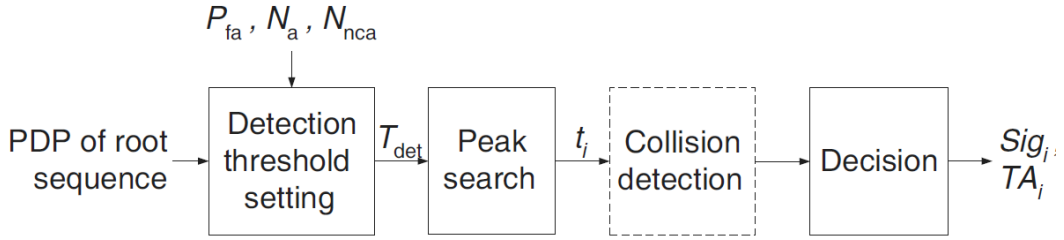


Figure 5.4: Signature detection per root sequence

The noise-floor threshold function collects the PDP output and estimates the absence or presence of an RA preamble by predefined threshold level. If the noise-floor threshold function detects the existence of RA preamble in received signal, peak searching function estimates preamble ID and propagation delay. Due to the unique correlation properties of ZC sequence as described previously, the preamble ID can be indicated by the peak position information and its cyclic shift value  $C_v$ . If the RA preamble is received with certain amount of propagation delay, the peak position information is effected by not only  $C_v$  but also the amount of delay. As described in Figure:??, the position of the peak is delayed in temporal domain by the quantity of propagation delay. According to this, the preamble detection module can estimate Preamble ID and its propagation delay exactly if the quantity of propagation delay in time domain is less than unit cyclic shift value.

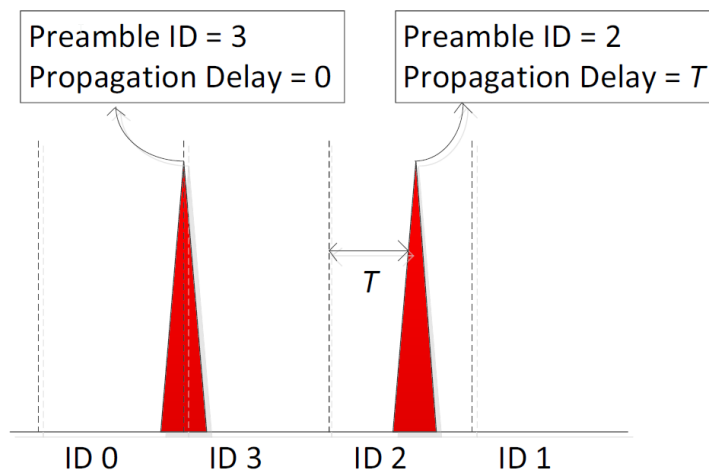


Figure 5.5: PRACH preamble detection



### 5.2.3 Noise floor estimation and threshold calculation

Noise floor can be calculated by considering transmission of only Gaussian noise, in the absence of preamble. The noise floor can be estimated as follows

$$\gamma(n) = \frac{1}{N_s} \sum_{i=0}^{N_s-1} z_{nca}(i) \quad (5.5)$$

where  $N_s$  is the number of samples in the search window, and  $z_{nca}(i)$  is given by the following expression

$$z_{nca}(i) = \sum_{a=1}^{N_a} \sum_{m=0}^{N_{nca}-1} |z_a^m(i)|^2 \quad (5.6)$$

where  $N_a$  is the number of antennas,  $N_{nca}$  is the number of additional non-coherent accumulations(e.g in case of sequence repetition preamble format) and  $|z_a^m(i)|^2$  is the PDP output for a particular antenna.  $z_{nca}(i)$  follows a central chi-square distribution with  $2N = 2N_a \cdot N_{nca}$  degrees of freedom with Cumulative Density Function  $F(T_{det}) = 1 - p_{fa}(T_{det})^{N_s}$  where  $N_s$  is number of samples in search window and  $T_{det}$  is the desired absolute threshold. The target false alarm probability  $p_{fa}(T_{det})$  drives the setting of the detection threshold  $T_{det}$  (The initial absolute threshold value is computed using an initial noise floor estimated by averaging across all search window samples). It is worth noticing that instead of the absolute threshold we can consider the threshold  $T_r$  relative to the noise floor  $\gamma(n)$  as follows:

$$T_r = T_{det}/\gamma(n) \quad (5.7)$$

This removes the dependency of  $F(T_r)$  on the noise variance:

$$F(T_r) = 1 - e^{-N_a \cdot N_{nca} T_r} \sum_{k=0}^{N_a \cdot N_{nca} - 1} \frac{1}{k!} (N_a \cdot N_{nca} T_r)^k \quad (5.8)$$

As a result, the relative detection threshold can be precomputed and stored.  $F(T_r)$  refers to the probability of PDP output samples (which in this case is obtained by just transmitting noise) less than relative threshold  $T_r$  and  $1 - F(T_r)$  gives probability of false alarm. The target false alarm probability drives the setting of absolute threshold  $T_{det}$ .

# Chapter 6

## Results

Link level simulations have been carried out for evaluating the performance of the algorithms. The proposed algorithms have also been applied to real time RF captured data from MW1000 test bed to verify the applicability of the algorithms in real time. The 20 MHz LTE system was considered, with a sampling frequency of  $f_s = 30.72\text{MHz}$ ,  $N = 2048$ -point FFT/IFFT, 144-sample CP and a 15kHz subcarrier spacing. The maximum channel delay spread was  $1.07\mu\text{s}$ , corresponding to 32 channel taps by considering system sampling frequency  $f_s$ . A frequency offset of 127kHz, which corresponds to  $\epsilon = 8.47$  has been considered. Only one antenna at the transmitter and receiver has been considered.

Figure ?? shows the simulation results of time domain correlation for PSS detection for one complete radio frame at SNR=0dB with two interferences considered with powers  $-2\text{dB}$  and  $-3\text{dB}$ . In this figure magnitude of correlation is plotted against sample location corresponding to single radio frame. Further it can be observed from Figure ?? that location of both the PSS in the given radio frame can be roughly estimated from the two dominant peaks. Whereas Figure ?? shows the time domain correlation for PSS detection for a real time RF captured signal from MW 1000 test bed. The received signal strength is 25mW which corresponds to  $-16\text{dB}$ . Sample location represents the time domain sample index while considering only one radio frame.

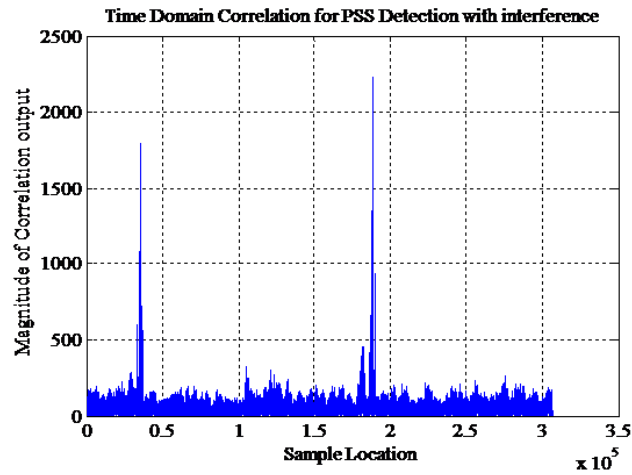


Figure 6.1: Simulation result of time domain correlation for PSS detection with interference

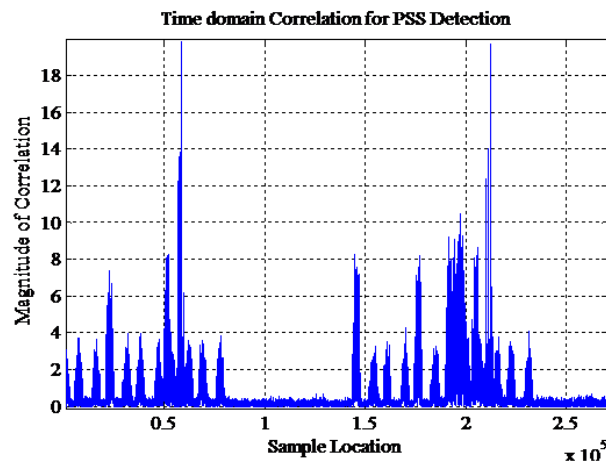


Figure 6.2: Time domain correlation for PSS detection for real time captured signal

Figure ?? illustrates the time coarse estimation based on Cyclic Prefix(CP) correlation. The magnitude of the CP correlation is plotted against the relative position from the estimation of the PSS location obtained from the time domain correlation for PSS detection as shown in Figure ?. Similarly Figure ? represents the CP correlation for a real time RF captured signal from MW 1000 test bed. The location corresponds to the CP correlation peak value as shown in the Figure ? and Figure ? gives the position where CP of the OFDM signal corresponding to PSS actually starts. Once the starting location of CP is obtained PSS and hence SSS can be obtained based on their known relative positions in terms of number of OFDM symbols.

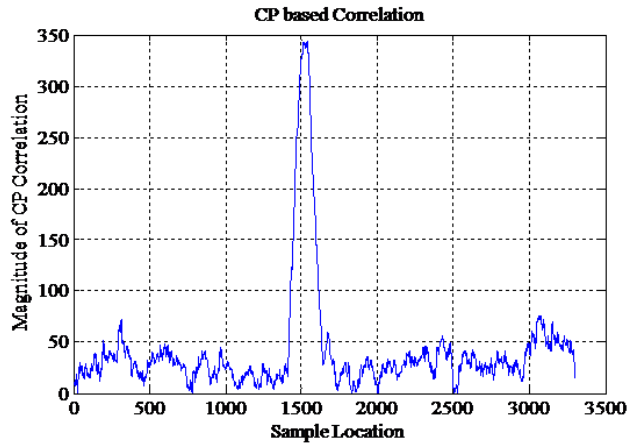


Figure 6.3: CP based correlation for simulated data

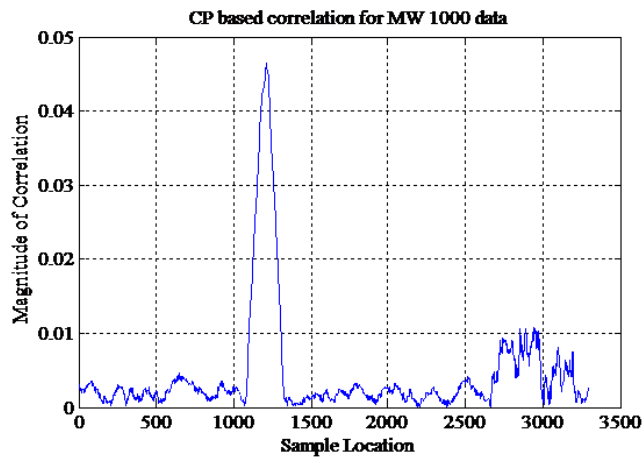


Figure 6.4: CP based correlation for real time RF captured data

2D-MMSE channel estimation is also performed on both PSS and SSS after detecting the correct cell-ID, to compare the results to that of an ideal case. Figure ?? represents the ideal constellation plot for PSS ZC-sequence in frequency domain. Figure ?? illustrates the PSS ZC-sequence constellation plot in frequency domain obtained after channel estimation for the real time captured data from MW 1000 test bed. Figure ?? represents the ideal constellation plot for SSS in frequency domain which is nothing but BPSK modulation. Figure ?? gives the constellation plot for the SSS in frequency domain after performing channel estimation on real time RF captured signal.

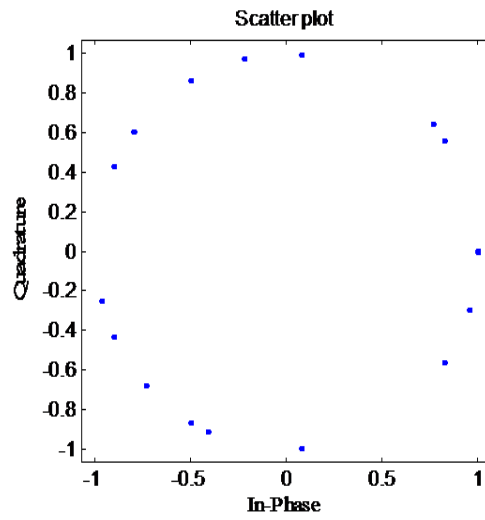


Figure 6.5: Ideal Constellation plot for PSS ZC-sequence in frequency domain

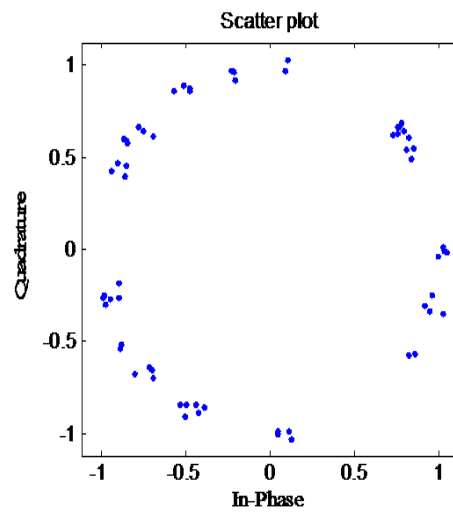


Figure 6.6: Received constellation plot for PSS ZC-sequence for real time RF captured data

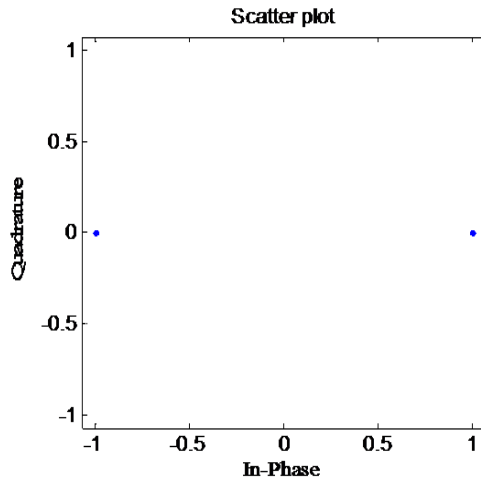


Figure 6.7: Ideal constellation plot for SSS signal in frequency domain

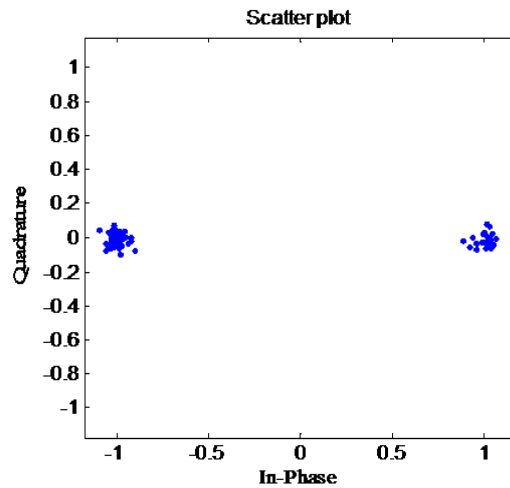


Figure 6.8: Received constellation plot for SSS signal for real time RF captured signal

Figure ?? illustrates the detection of multiple UE's transmitting different PRACH preamble over real time wireless channel. In this figure Power delay profile (PDP) is plotted against the samples in time domain related to the length of ZC sequence which is equal to 839 in case of PRACH transmission. There are 9 different UE's transmitting 9 different preambles which have been transmitted and captured over real time channel. Figure ?? shows detection of all the 9 different preambles, corresponding to 9 different peaks. The preamble number can be obtained based on the location of the preamble peaks.

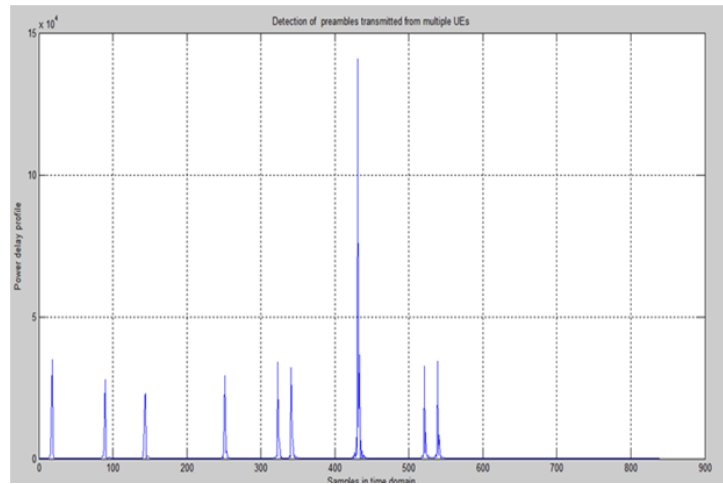


Figure 6.9: Multiple UE's detection for PRACH transmission over real time channel

# Chapter 7

## Conclusions and Future Work

For a 3GPP LTE receiver, a cross-correlation approach is proposed to estimate the sector-ID from PSS in time domain instead of shifting time window each time by one sample converting it into frequency domain and performing cross-correlation of Zadoff-chu sequence in frequency domain whereas frequency domain correlation needs to be performed on SSS to estimate group ID and hence enable cell identification. It also provides a reliable estimate of the beginning of frame and estimates fractional frequency offsets based on cyclic prefix correlation. However, for timing acquisition the low-complexity cyclic prefix based autocorrelation should be preferred, as it is not influenced by frequency errors. In this work, estimation of large frequency offset and cell search are jointly performed with the secondary synchronization signal. Uplink synchronization has been obtained based on either by hybrid time frequency domain approach or full frequency domain approach followed for PRACH preamble detection and estimating the propagation delays of multiple UE's. The complete procedure enables a robust connection to the base station at a reasonable implementation complexity.

Future work includes correction of the FFT window drift caused by the sampling clock offset. Sampling clock offset errors include the clock phase errors and the clock frequency error. The clock phase error are similar to the symbol timing error and the clock phase error can be treated as a kind of the symbol timing error. The sampling clock frequency errors can cause the ICI. The sampling clock frequency errors can be detected along with carrier frequency offset from the scheme mentioned in this thesis. The clock phase error, which leads to FFT window drift needs to be tracked and has to be compensated in order to obtain perfect timing synchronization.



# References

- [1] 3GPP TS36-211(v9.1.0), “Physical channels and modulation”, Mar. 2010
- [2] J.J van de Beek, M. Sandell and P. O Borjesson, “ML Estimation of Time and Frequency Offset in OFDM Systems”, *IEEE Trans. Signal processing*, vol. 45, no. 7, July 1997.
- [3] L. J. Cimini, “Analysis and simulation of a digital mobile channel using orthogonal frequency division multiplexing”, *IEEE Trans. Commun.*, vol. 33, pp. 665-675, July 1985.
- [4] K. Manolakis, et al., “A closed concept for synchronization and cell search in 3GPP LTE systems”, in *Proc. IEEE Wireless Communications and Networking Conference*, April 2009.
- [5] P.-Y. Tsai and H.-W. Chang, “A new cell search scheme in 3GPP long term evolution downlink OFDMA systems”, in *Proc. International Conference on Wireless Communications and Signal Processing*, Nov. 2009.
- [6] H.-G. Park, I.-K. Kim and Y. -S. Kim, “Efficient coherent neighbour cell search for synchronous 3GPP LTE system”, *IET Electron. Lett.*, 2008, 44, (21), pp. 1267-1268.
- [7] J. J. van de Beek, M. Sandell, M. Isaksson, and P. O. Borjesson, “ Lowcomplex frame synchronization in OFDM systems”, in *Proc. IEEE Int. Conf. Universal Personal Commun.*, Nov. 1995, pp. 982-986.
- [8] K. Manolakis and V. Jungnickel, “Synchronization and Cell Search for 3GPP LTE”, *13th International OFDM Workshop (InOWo08)*, August 2008.
- [9] M.Sandell, J.J. v.d. Beek and P.O.Borjesson, Timing and Frequency Synchronization in OFDM Systems Using the Cyclic Prefix, *Proc. IEEE Int. Symp. Synchronization*, Essen, Germany, Dec. 1995.

- [10] Yinigmin Tsai and Guodong Zhang, “Time and Frequency Synchronization for 3GPP LTE Long Term Evolution Systems, *IEEE Vehicular Technology Conference*, 65th VTC2007-Spring, April 2007.
- [11] M. Speth, F. Classen, and H. Meyr, “Frame synchronization of OFDM systems in frequency selective fading channels”, in *Proc. VTC97*, pp. 1807-1811.
- [12] J. G. Proakis, *Digital Communications*, McGraw-Hill, 4th edition, 2001.
- [13] . F. Khan, *LTE for 4G Mobile Broadband: Air Interface Technologies and Performance*, Cambridge University Press, 2009.
- [14] M. Speth, S.A. Fechtel, G. Fock and H. Meyr, “Optimum Receiver Design for Wireless Broad-Band Systems Using OFDM - Part I, *IEEE Transactions on Communications*, Vol.47, No. 11, November 1999.
- [15] M. Speth, S.A. Fechtel, G. Fock and H. Meyr, “Optimum Receiver Design for Wireless Broad-Band Systems Using OFDM - Part II, *IEEE Transactions on Communications*, Vol.49, No. 4, April 2001.
- [16] S. B. Weinstein and P. M. Ebert, “Data Transmission by Frequency-Division Multiplexing using the Discrete Fourier Transform”, *IEEE Trans. on Communications*, Vol. 19, pp. 628634, October 1971.
- [17] S. Sesia, I. Toufik, and M. Baker, *LTE- The UMTS Long Term Evolution From theory to Practice*, John Wiley and Sons Ltd., 2009.
- [18] W. C. Jakes, *Microwave Mobile Communications*, Wiley, 1974.
- [19] P. H. Moose, “A technique for orthogonal frequency division multiplexing frequency offset correction, *IEEE Trans. Commun.*, vol. 42, pp. 29082914, Oct. 1994.
- [20] B. Yang, Khaled B. Lataef, Roger S. Cheng, Z. Chao, “Timing Recovery for OFDM Transmission, *IEEE Journal on Communications*, Vol. 18, No. 11, November 2000.
- [21] Erik Dahlman, Stefan Parkvall and Per Beming, “3G Evolution HSPA and LTE for Mobile Broadband, Academic Press, 2008.